

**FABRICATION AND INVITRO CHARACTERIZATION OF
BIOACTIVE GLASS / NANO-HYDROXYAPATITE
REINFORCED ELECTROSPUN POLYCAPROLACTONE
COMPOSITE MEMBRANES FOR PERIODONTAL
TISSUE ENGINEERING**

DISSERTATION

Submitted to The Tamil Nadu Dr. M.G.R Medical University
in partial fulfillment of the requirement for the degree of

MASTER OF DENTAL SURGERY



BRANCH II

PERIODONTOLOGY

2014 - 2017

**SREE MOOKAMBIKA INSTITUTE OF DENTAL
SCIENCES, KULASEKHARAM**

**ENDORSEMENT BY THE PRINCIPAL / HEAD OF THE
INSTITUTION**

This is to certify that the dissertation entitled "Fabrication and *invitro* Characterization of Bioactive glass / Nano-Hydroxyapatite Reinforced Electrospun Polycaprolactone Composite Membranes For Periodontal Tissue Engineering" is a bonafide research work done by **Dr. Vishnu J.S** under the guidance of **Dr. Elizabeth Koshi, M.D.S**, Head of the Department, of Periodontics, Sree Mookambika Institute of Dental Sciences, Kulasekharam.

Dr. Elizabeth Koshi, MDS,

PRINCIPAL

Sree Mookambika Institute of Dental Sciences,
V.P.M Hospital Complex,
Padanilam,
Kulasekharam,
Kanyakumari District,
Tamil Nadu - 629161

CERTIFICATE

This is to certify that the dissertation titled "Fabrication and *invitro* Characterization of Bioactive glass/Nano-Hydroxyapatite Reinforced Electrospun Polycaprolactone Composite Membranes For Periodontal Tissue Engineering" is a bonafide record of the work done by **Dr. Vishnu J.S**, under our guidance during his postgraduate study period of 2014-2017. The dissertation is submitted to **THE TAMIL NADU DR. M.G.R MEDICAL UNIVERSITY, CHENNAI**, in partial fulfillment of the requirement for the Degree of **MASTER OF DENTAL SURGERY IN PERIODONTOLOGY, BRANCH II**. It has not been submitted (partial or full) for the award of any other degree or diploma.

GUIDE

Dr. Elizabeth Koshi, MDS
Head of the Department,
Department of Periodontics
Sree Mookambika Institute of Dental
Sciences, Kulasekharam 629161

CO-GUIDE

Dr Arun Sadasivan, MDS
Professor,
Department of Periodontics
Sree Mookambika Institute of Dental
Sciences, Kulasekharam 629161

ACKNOWLEDGEMENT

Effort is like toothpaste, you can always squeeze out just a little bit more-

Howard Farran

I am ever grateful to God, the Creator and the Guardian, and to whom I owe my very existence.

This thesis owes its existence to the help, support and inspiration of several people. Firstly, I must offer my profoundest gratitude and sincere appreciation to **Dr. Elizabeth Koshi MDS**, Principal, Professor & Head, Department of Periodontics for her guidance during my research. Her support and inspiring suggestions have been precious for the development of this thesis content.

I am very much indebted to Professor. **Dr. Arun Sadasivan MDS**, from finding an appropriate subject in the beginning to the process of writing thesis, sir offered his unreserved help and guidance and lead me to finish my thesis systematically. His words can always inspire me and bring me to a higher level of thinking. What I learn from him is not just how to write a thesis to meet the graduation requirement, but how to view this world from a new perspective. Without his kind and patient instruction, it is impossible for me to finish this thesis.

I would like to acknowledge the help and support given by **Dr. C. K. Velayuthan Nair, MBBS, MS.,** Chairman, **Dr. Rema V Nair MBBS, MD, DGO.,** Director, **Dr. Vinu Gopinath MS, Mch.** and **Dr. R.V. Mookambika MD, DM.,** without which my study would not have been possible.

I would like to acknowledge **Dr. Shilpa Jayakumar MDS, Dr. Nikhil Das MDS**, senior lecturers in the Department of Periodontics, for their constant enthusiasm and support showed in me completing this work.

It is my utmost privilege to acknowledge the debt I owe to **Dr. P. R. Harikrishna Varma**, Head of SCTIMST, Poojappura, Trivandrum, **Dr. Ramesh. P, Dr. Remya K.R, Mr. Nishad, Mr. Suresh Sivadasan** of Biomaterial Technology wing, SCTIMST, **Dr. Athira Jayakumar**, Ph.D Student of Biochemistry wing, Fine arts college, Trivandrum, **Dr. Rajesh**, Head of Biogenix Research Centre, Trivandrum for their technical help, constant encouragement and liberty they provided me without which my study would not have been possible.

I am thankful to **Dr. Muralidharan Nair** for providing me with this timely statistical analysis involved in this study.

I am also indebted to my friends, **Dr. Sheethal V. Menon, Dr. Shamna, Dr. Anju, Dr. Blessing** and **Dr. Anina** who squeeze time from their busy schedule to help me finish my thesis. All of them are busy with their own thesis and work, but they are willing to give their helping hands as soon as I am in need. I would like to express my special thanks to **Dr. Blessing** for being a great soul. He is always ready to help with a smile and always comes up with critical questions and constructive advice to improve my thesis. I cannot finish my thesis so soon without their kind assistance and encouragement.

I am thankful to my wife **Dr. Aswathy Krishna** for her constant encouragement, appreciation and support all through my study works.

With deep sense of gratitude and love to my parents who provide a carefree environment for me, so that I can concentrate on my study. Although they hardly understand what writing thesis is and what I research on, my parents are willing to support any decision I make. Even though I cannot make money as other boys in my age, they never complain. They tell me that all I need to do is focus on my study and leave other things to them. I am so lucky to have them be my parents.

CONTENTS

Sl. No	Index	Page No
1.	List of Abbreviations	i
2.	List of Tables	iii
3.	List of Graphs	v
4.	List of color plates	vi
5.	List of Annexure	viii
6.	Abstract	ix
7.	Introduction	1
8.	Aims and objectives	5
9.	Review of literature	6
10.	Materials and Methods	22
11.	Results and Observations	30
12.	Discussion	57
13.	Summary	69
14.	Conclusion	70
15.	Bibliography	xi
16.	Annexure	

LIST OF ABBREVIATIONS

BG	-	Bioactive Glass
E-spinning	-	Electrospinning
ECM	-	Extracellular Matrix
E-PTFE	-	Expanded- Poly Tetra Fluoro Ethylene
FTIR	-	Fourier Transformation Infrared Spectroscopy
GTR	-	Guided Tissue Regeneration
Kv	-	Kilovolt
µg	-	Microgram
Mg	-	Milligram
mm	-	Millimetre
Mwt	-	Molecular weight
nHAP	-	Nanohydroxyapatite
OD	-	Optical Density
PDL	-	Periodontal Ligament
PBS	-	Phosphate Buffered saline
PTFE	-	Poly Tetra Fluoro Ethylene
PCL	-	Polycaprolactone

PCL+BG2%	-	Polycaprolactone blended with 2wt % of Bioactive glass
PCL+BG5%	-	Polycaprolactone blended with 5wt % of Bioactive glass
PCL+BG10%	-	Polycaprolactone blended with 10wt % of Bioactive glass
PCL+BG15%	-	Polycaprolactone blended with 15wt % of Bioactive glass
PCL+HA2%	-	Polycaprolactone blended with 2wt % of Nano Hydroxyapatite
PCL+HA5%	-	Polycaprolactone blended with 5wt % of Nano Hydroxyapatite
PCL+HA10%	-	Polycaprolactone blended with 10wt % of Nano Hydroxyapatite
PCL+HA15%	-	Polycaprolactone blended with 15wt % of Nano Hydroxyapatite
PGA	-	Polyglycolic acid
SEM	-	Scanning Electron Microscope
TGA	-	Thermogravimetric analysis
3D	-	Three Dimensional
TE	-	Tissue Engineering

LIST OF TABLES

Table No	Title
Table 1	Comparison of Mean Fiber diameter between the groups
Table 2	Comparison of Mean Pore diameter between the groups
Table 3	Comparison of Initial Mean Tensile Strength between the groups
Table 4	Comparison of Mean Tensile strength between the groups at 14 days
Table 5	Comparison of Mean Tensile strength between the groups after 28 days
Table 6	Comparison of Mean Tensile strength within the groups at different time periods
Table 7	Comparison of Initial Mean Youngs modulus between the groups
Table 8	Comparison of Mean Youngs modulus between the groups at 14 days
Table 9	Comparison of Mean Youngs modulus between the groups after 28 days
Table 10	Comparison of Mean Youngs modulus within the groups at different time periods
Table 11	Comparison of Initial Mean Elongation at break between the groups
Table 12	Comparison of Mean Elongation at break between the groups after 14 days
Table 13	Comparison of Mean Elongation at break between the groups after 28 days
Table 14	Comparison of Mean Elongation at break within the groups at different time periods
Table 15	Comparison of Initial Mean Weight between the groups
Table 16	Comparison of Mean Weight loss between the groups after one month

Table 17	Comparison of Mean weight loss within the groups at different time periods
Table 18	Comparison of Initial Mean Thickness between the groups
Table 19	Comparison of Mean Thickness between the groups at 14 days
Table 20	Comparison of Mean Thickness between the groups after 28 days
Table 21	Comparison of Mean Thickness within the groups at different time periods
Table 22	Comparison of Percentage viability of cells between the groups at 24 hours

LIST OF GRAPHS

Graph No	Title
Graph 1	Comparison of Mean Fiber diameter between the groups
Graph 2	Comparison of Mean Pore diameter between the groups
Graph 3	Comparison of Mean Tensile strength within the groups at different time
Graph 4	Comparison of Mean Youngs modulus within the groups at different time periods
Graph 5	Comparison of Mean Elongation at break within the groups at different time periods
Graph 6	Comparison of Mean weight loss within the groups at different time periods
Graph 7	Comparison of Mean Thickness within the groups at different time periods
Graph8	FTIR analysis of Hydroxyapatite
Graph 9	FTIR analysis of BG
Graph 10	FTIR analysis of PCL + HA
Graph 11	FTIR ANALYSIS of PCL + BG
Graph 12	TGA of PCL + BG
Graph 13	TGA of PCL + HA
Graph 14	Comparison of Percentage viability of cells between the groups at 24 hours

LIST OF COLOR PLATES

Color plate No.	Title
1	Polycaprolactone polymer Pellets
2	Bioactive glass powder
3a	Dichloromethane
3b	Dimethyl formamide
4	Electrospinning setup
5	Electronic weighing machine
6	Measuring cylinder 25 ml
7	Automatic Stirrer
8	10ml syringes with 21 gauge needle
9	Vaccum oven
10 a	Specimen Cutting Dies
10 b	Specimen Cutting Dies
11	Thickness Gauge
12	Universal testing machine (Instron 3345, single column, UK)
13	Scanning Electron Microscope[Hitachi-model-S-2400, JEOL, JSM-6390, model 7582, Japan]
14	FTIR spectrometer
15	Thermogravimetric analyzer[Shimadzu TGA-50 (Shimadzu Corporation, Kyoto, Japan)]

16	Phase contrast microscope(Olympus CKX41)
17	Incubator
18	Clear homogenous solution of Polymer and Bioactive Material
19	Electrospun Nanofibrous sheets
20	Dumpbell shaped specimen
21	Measuring Mechanical Properties
22	Measuring thickness using Thickness Gauge
23	Samples immersed in PBS
24	Samples placed in Incubator
25	Images 1-27 (SEM images of fabricated GTR membranes)
26	Images 28-39 (Images of direct contact and MTT assay of fabricated GTR Membranes with L-929 mouse fibroblasts)

LIST OF ANNEXURE

Annexure No.	Title
Annexure-1	Permission letter from SCTIMST, Trivandrum
Annexure-2	Certificate from Institutional Research Committee

ABSTRACT

Background

Periodontitis is a chronic inflammatory disorder that can lead to the destruction of the periodontal tissues and ultimately tooth loss. To date, flap debridement and/or flap curettage and periodontal regenerative therapy with membranes and bone grafting materials have been employed with distinct levels of clinical success. Current resorbable and non-resorbable membranes act as a physical barrier to avoid connective and epithelial tissue downgrowth into the defect, favouring the regeneration of periodontal tissues. These conventional membranes possess many structural, mechanical, and bio-functional limitations and the “ideal” membrane for use in periodontal regenerative therapy has yet to be developed. Based on a bioactive material approach, we have hypothesized that the next-generation of guided tissue regeneration (GTR) membranes for periodontal tissue engineering will be a biologically active, spatially designed nanofibrous biomaterial that closely mimics the native extra-cellular matrix (ECM).

Aim of the study

The aim of the study was to Fabricate Bioceramic Reinforced Nanofibrous GTR membranes by the method of Electrospinning and to compare their invitro characteristics.

Materials and Methods

GTR membranes made of Polycaprolactone with a molecular weight of 80,000 reinforced with different weight concentrations of Nano Hydroxyapatite /Bioactive Glass [2%,5%,10%,15%] is fabricated by the method of Electrospinning. After fabrication, their invitro properties are evaluated.

Morphology of the membranes such as Fibre diameter and Pore diameter was evaluated using SEM, Mechanical properties such as Tensile strength, Young's modulus and Elongation at break are evaluated using Instron 3345 universal testing machine initially and after one month of *In vitro* degradation in PBS. Weight loss and thickness of the fabricated membranes were evaluated. For chemical and thermal stability evaluation, FTIR and TGA were performed. Percentage of viable cells were evaluated using L-929 mouse fibroblasts.

Results

All the Electrospun nanofibrous membranes possessed excellent Mechanical properties initially and after one month of degradation in PBS. Moreover none of the membranes found to be cytotoxic at lower concentrations and higher concentrations. On comparing the overall properties, PCL+BG2% exhibited superior cell attachment and percentage of viable cells, increased fiber and pore diameter which satisfies the ideal properties needed for GTR membranes.

Conclusion

From the observations of the study it was concluded that the composite nanofibrous membranes prepared by Electrospinning is suitable for the use as a GTR membrane and it is a useful prototype for further development of a final membrane for clinical use.

INTRODUCTION

Periodontitis, which is bacterially induced, can be defined as a chronic inflammatory disease initiated by dental plaque biofilm and perpetuated by a deregulated immune response usually accompanied by gingivitis resulting in irreversible destruction of the supporting tissues surrounding the tooth, including the periodontal ligament, cementum and the alveolar bone finally causing tooth loss.¹ The goals of periodontal therapy are to cure the disease, to prevent disease recurrence, that is, maintain periodontal health and to restore periodontal tissues lost through the disease.² Conventional periodontal surgical treatment modalities (surgical debridement and resective procedures) have been established as effective means of treating periodontal disease and arresting its progression. These methods typically heal by repair, with a combination of connective tissue adhesion/attachment or formation of a long junctional epithelium.³ To obtain good stability and predictability after therapy, periodontal regeneration of destroyed tissue, which is characterized by de novo formation of cementum, a functionally organized PDL, alveolar bone, and gingiva, is desirable. The desire to induce the complete regeneration of periodontal tissue has inspired the introduction of Guided Tissue Regeneration technique.⁴

The term “Guided Tissue Regeneration (GTR)” was given by Gottlow in 1986. The 1996 World Workshop in Periodontics defined GTR as “procedures attempting to regenerate lost periodontal structures through differential tissue responses”. The principle of GTR was based on Melchers hypothesis [1976] which states that certain cell populations residing in the periodontium have the potential to create new cementum, alveolar bone and PDL, when they are provided the opportunity to populate the periodontal wound.⁵ GTR employs a barrier membrane

around the periodontal defect to prevent epithelial downgrowth and fibroblast transgrowth into the wound space, thereby maintaining a space for true periodontal tissue regeneration. The barrier membranes used for GTR can be broadly divided into three generations of membranes.

The first generation of barrier membranes were non resorbable membranes such as titanium reinforced Expanded poly tetra fluoro ethylene[e-PTFE], high-density-PTFE, or titanium mesh which are aimed to achieve a suitable combination of physical properties to match those of the replaced tissue with a minimal toxic response in the host. In the first GTR attempts, a bacterial filter produced from cellulose acetate (Millipore) was used as an occlusive membrane by Nyman et al in 1982. The major drawback is the need for second surgery for the removal of the membrane.

The second generation of barrier membranes was designed to be resorbable to avoid the need for surgical removal. There are two broad categories of bioresorbable membranes: the natural and the synthetic membranes. Natural membranes are made of collagen or chitosan. Synthetic barrier materials made of polyesters (e.g, poly(glycolic acid) (PGA), poly(lactic acid) (PLA), poly(-caprolactone) (PCL), and their copolymers) were used. Several complications, such as early degradation, epithelial downgrowth along the material, premature loss of material, tissue reactions and lack of control over the rate of membrane resorption were reported as the drawbacks of second generation barrier membranes.⁶

Third generation barrier membranes are developed based on the concept of Tissue Engineering [TE]. TE is a multi-disciplinary field, which aims to apply

innovative biomaterials to replace or restore ill or damaged tissues of the human body, such as skin and bones.⁷ The triad for conventional cell-based TE involves cells, signaling molecules, and scaffold/supporting matrices. In this triad, the role of the scaffold is the “niche” of cells, and facilitates the attachment, migration, proliferation, and three-dimensional (3D) spatial organization of the cell population that defines the shape of the tissue that needs regeneration.⁸ Third-generation membranes have evolved, which not only act as barriers but also as delivery devices to release specific agents such as bioactive materials ,antibiotics, growth factors, adhesion factors, etc., at the wound site on a time or need basis in order to orchestrate and direct natural wound healing in a better way .

Briefly they may be considered into the following sub divisions:

- 1) Barrier membranes with Antimicrobial activity
- 2) Barrier membranes with Bioactive materials
- 3) Barrier membranes with Growth Factor release

A number of novel approaches have been developed for the fabrication of biomaterial-based 3D scaffolds .Currently, some of the most promising scaffolding materials for application in bone tissue engineering are Hydroxyapatites[HA], Bioactive glasses[BG] and related biodegradable polymer materials(e.g. PCL, PGA etc). These scaffolds are highly porous, 3D structures exhibiting tailored porosity, pore size and interconnectivity.⁹ There is a high number of polymer bioceramic composite membrane manufacturing techniques, such as solvent casting, particulate leaching, Three dimensional printing, Thermally induced phase separation (TIPS). The development of nanofibers has enhanced the scope for fabricating bioactive

membranes that can potentially mimic the architecture of natural human tissue at the nanometer scale. The high surface area to volume ratio of the nanofibers combined with their microporous structure favors cell adhesion, proliferation, migration, and differentiation, all of which are highly desired properties for tissue engineering applications. Therefore, current research in this area is driven towards the fabrication, characterization, and applications of nanofibrous systems for TE.¹⁰ Phase separation, Self assembly and Electrospinning [E-spinning] are the three techniques available for fabricating nano structured fibers with variable morphological characters.¹¹ Of these, E-spinning is the most widely studied technique and also seems to exhibit the most promising results for TE applications.¹⁰ The E-spinning technique has demonstrated great potential for processing membranes for periodontal regeneration. E-spinning produces a biocompatible and degradable natural or synthetic polymers that normally resembles the arrangement of the native extracellular matrix (ECM) ⁶. Although the concept of E-spinning or electrospraying has been known for more than a century, polymeric nanofibers produced by E-spinning have become a topic of great interest only in the past decade.¹⁰ Electrospun composite membranes can be tailored with desired new functions by selecting a suitable material or composite and by adjusting the component ratio, fibre diameter and morphology through process parameters.¹²

Hence in this study, an attempt is being made to fabricate GTR membranes of resorbable polymer Polycaprolactone blended with Bioactive glass and Hydroxyapatite of varying weight concentrations using Electrospinning technique and to compare their invitro properties.

AIMS & OBJECTIVES

Aim of the study

The aim of the study was to fabricate Bioceramic reinforced nanofibrous GTR membranes by the method of Electrospinning and to compare their invitro characteristics.

Objectives of the study

- To fabricate the GTR membrane by incorporating varying concentrations of Bioactive glass [BG-2wt%, 5wt%, 10wt% & 15wt%] and Hydroxyapatite [HA-2wt%, 5wt%, 10wt% & 15wt%] into Polycaprolactone [PCL] polymer by the method of Electro spinning.
- To characterize and compare the invitro Mechanical, Thermal and Chemical properties of GTR membranes after their fabrication
- To compare the intergroup and intragroup invitro properties exhibited by the membranes
- To assess the cytotoxicity of the fabricated membranes.
- To evaluate the Mechanical properties of each membrane after one month of degradation under Phosphate buffered saline[PBS].

REVIEW OF LITERATURE

Regeneration of the reduced periodontium is the ideal goal in periodontal therapy. By definition, successful periodontal regeneration is the simultaneous regeneration of cementum, PDL, and alveolar bone, so that the form and function of the lost structures are restored. In 1976 Melcher formulated a hypothesis which suggested that, under physiological conditions, only cells from periodontal ligament can synthesize and secrete cementum to attach newly- synthesised collagen fibres to tooth. This hypothesis was experimentally and histologically verified by Karring et al. The necessity for exclusion of epithelial and connective tissue cells of the gingiva from the wound led to the development and application of Guided Tissue Regeneration (GTR) membranes.¹³ There are different generations of GTR Membranes .The most recent generation of GTR Membrane is based on degradable polymer Polyglycolide, polycaprolactone, polylactic acid incorporated with bioactive material such as hydroxy apatite, Bioactive glass, calcium sulphate etc. Among these biodegradable polymer, Polycaprolactone shown great promise as a barrier membrane for tissue engineering.¹⁴

Polycaprolactone[PCL]

Polycaprolactone (PCL) is a family member of biodegradable aliphatic polyesters which have found important use as biomaterials in prosthetics, sutures, and drug delivery systems. As a commercial material, the main attractions of PCL are¹⁵

1. Its approval by the Food and Drug Administration (FDA) for use in humans,
2. Its biodegradability
3. Its compatibility with a wide range of other polymers

4. Its good processibility which enables fabrication of a variety of structures and forms
5. Its ease of melt processing due to its high thermal stability and
6. Its relatively low cost.

PCL can be easily fabricated into a material possessing the desired toughness.¹⁶ Overall, PCL has been proven effective for the use in tissue engineering settings. The biocompatibility with the body has been proven. The fact the polymer is bioresorbable helps with numerous tissue engineering factors. With bioresorbable polymers, the fibers provide a back support for the cell growth. After time in the body, the fibers essentially dissolve and leave the cell growth (sometimes in tissue form) in a pure form within the body. Another positive of using polymer, like PCL, is that the body will be more apt to accept the fibers and not cause a potentially devastating immune response cascade.¹⁷

However, this material alone without additives demonstrates low mechanical resistance to compressive loading, hydrophobicity, and low bioactivity. To counter these problems, Ma et al in 2001 suggested addition of bioactive ceramics to biodegradable polymer composite materials. These new materials demonstrated superior properties including improvement in material strength, stiffness, biodegradability, osteoconductivity, and bioactivity. In addition, polymer/bioactive ceramic composite scaffolds have structures that resemble bone, where the inorganic component of these scaffolds mimics the hydroxycarbonate-apatite (HCA) motifs while the polymer component mimics the collagen-rich extracellular matrix.¹⁶

Although numerous membrane materials have been investigated, few studies have focused on the technique of membrane preparation. So far, most GTR membranes are made in the shape of porous form, created by traditional methods such as particulate leaching, solvent casting or gas foaming. Recently, a new technique has been introduced, which is called Electrospinning, and allows the preparation of thin fibrous membranes. Electrospinning makes use of a high electric voltage to draw polymer solutions/melts into a whipped jet, which becomes ultrafine fibers after drying in air. Fibers obtained from electrospinning are in the range of 50 nm to a few microns in diameter and generally collected in the form of a non-woven structure. It has already been shown that electrospun membranes have the potential to promote osteoblastic cell function and bone regeneration. More importantly, the pore size of the electrospun membranes in general is less than the average cell size, and previous studies have shown that such small pores do not allow cell penetration.¹⁸

PCL-HA COMPOSITE MEMBRANES

Gurbuz et al in 2016¹⁹ fabricated and characterized Multi-layered functional membranes[MLMs] for periodontal regeneration by combining electrospinning and solvent casting/particulate leaching methods. MLMs possess three layers of different functional properties; poly (caprolactone) (PCL)/nano-hydroxyapatite core layer and PCL/collagen, PCL/collagen-bone morphogenic protein 7 (BMP 7) outer layers on each side of the core layer. MC3T3-E1 cell culture tests showed that osteoblastic differentiation was enhanced on PCL/collagen BMP 7 layer. The authors concluded that this facile method presents great potential for fabrication of multi-functional barrier membranes for periodontal regeneration as well as scaffolds possessing different properties to mimic complex extra cellular matrix structures with stable integrity.

Mario et al in 2015²⁰ fabricated microporous membranes based on poly(ϵ -caprolactone) (PCL) and PCL functionalized with amine (PCL-DMAEA) or anhydride groups (PCL-MAGMA) that was realized by solvent–non solvent phase inversion and proposed for use in Guided Tissue Regeneration (GTR). Nano whiskers of hydroxyapatite (HA) were also incorporated in the polymer matrix to realize nanocomposite membranes. Scanning Electron Microscopy (SEM) showed improved interfacial adhesion with HA for functionalized polymers, and highlighted substantial differences in the porosity. A relationship between the developed porous structure of the membrane and the chemical nature of grafted groups was proposed. Compared to virgin PCL, hydrophilicity increases for functionalized PCL, while the addition of HA influences significantly the hydrophilic characteristics only in the case of virgin polymer. A significant increase of in vitro degradation rate was found for PCL-MAGMA based membranes, and at lower extent of PCL-DMAEA membranes. The novel materials were investigated regarding their potential as support for cell growth in bone repair using multipotent mesenchymal stromal cells (MSC) as a model. MSC plated onto the various membranes were analyzed in terms of adhesion, proliferation and osteogenic capacity that resulted to be related to chemical as well as porous structure. The authors concluded that PCL-DMAEA and the relative nanocomposite membranes are the most promising in terms of cell-biomaterial interactions which warrants its use in Guided tissue regeneration.

Remya et al in 2013²¹ fabricated Nanohydroxyapatite Incorporated Electrospun Polycaprolactone / Polycaprolactone - Polyethyleneglycol - Polycaprolactone blend Scaffold for Bone Tissue Engineering Applications. The study was a comparative evaluation of physical and biological properties of electrospun biodegradable fibrous

scaffolds based on polycaprolactone (PCL) and its blend with polycaprolactone–polyethyleneglycol–polycaprolactone (CEC) with and without nanohydroxyapatite (nHAP) particles. The fiber morphology, porosity, surface wettability, and mechanical properties of electrospun PCL were distinctly influenced by the presence of both copolymer CEC and nHAP. The degradation in hydrolytic media affected both morphological and mechanical properties of the scaffolds and the tensile strength decreased by 58% for PCL, 83% for PCL/CEC, 36% for PCL/nHAP and 75% for PCL/CEC/nHAP in 90 days of PBS ageing. MTT assay using mouse fibroblast L929 cells proved all the scaffolds to be non-cytotoxic. These results revealed that the potential of the cytocompatible PCL/CEC/nHAP scaffold for the fabrication of living bony constructs for tissue engineering applications.

Hassan et al in 2012²² prepared HA/PCL Scaffolds for tissue engineering. The wet slurry of HA was produced by mixing an acetone solution of calcium nitrate 4-hydrate with an aqueous solution of ammonium phosphate and ammonium carbonate with control pH of 11. The nano-emulsion was kept in freezer about one day and after that was kept in freeze drying machine about three days to obtain dry HA powder with low degree of agglomeration. The nanoparticles were studied under scanning electron microscopy (SEM). The polycaprolactone (PCL) and hydroxyapatite/ polycaprolactone (HA/PCL) composite scaffolds were produced using thermally induced phase separation (TIPS) technique. The scaffolds were studied under SEM and it was observed that both types of scaffolds had porous structures. The pore sizes of HA/PCL scaffold was slightly decreased compared to PCL scaffold. The authors concluded that both PCL and HA/PCL scaffolds showed promises for bone tissue engineering application.

Botino et al in 2007²³ fabricated a novel functionally graded membrane (FGM) via sequential multilayer electrospinning. The FGM consists of a core layer (CL) and two functional surface layers (SLs) interfacing with bone (nano-hydroxyapatite, n-HAp) and epithelial (metronidazole, MET) tissues. The CL comprises a neat polycaprolactone (PCL) layer surrounded by two composite layers composed of a protein/polymer ternary blend (PCL:PLA:GEL). Electrospinning parameters involved in fabrication of the individual layers (i.e. neat PCL, ternary blend, PLA:GEL + 10%n-HAp and PLA:GEL + 25%MET) were optimized to obtain fibrous layers free of beads. Morphology, structure and mechanical property studies were carried out on each electrospun layer. The individual fiber morphology and roughness of the functional SLs, which are the n-HAp containing and drug-incorporating layers were evaluated by atomic force microscopy. The CL structure demonstrated higher strength (8.7 MPa) and a more elastic behavior (strain at break 357%) compared with the FGM (3.5 MPa, 297%).the authors conclude that incorporation of n-HAp to enhance osteoconductive behavior and MET to combat periodontal pathogens led to a novel FGM that holds promise at solving the drawbacks of currently available membranes.

Shalumon et al in 2011²⁴ conducted a study to evaluate the effect of Electrospun Multi-scale Poly(caprolactone) Fibrous Scaffolds for Tissue Engineering. Electrospun nano, micro and micro/nano (multiscale) poly(caprolactone) (PCL) fibrous scaffolds with and without nano hydroxyapatite (nHAp) was prepared. All the scaffolds were evaluated for its spectroscopic, morphological, mechanical, thermal, cell attachment and protein adsorption properties. The cell attachment studies showed that cell activity on the nano-fibrous,

as well as multi-scale scaffolds with and without nHAp was higher compared to micro-fibrous scaffolds. The cell activity, proliferation and total protein adsorption on the nano-fibers/nano-fibers with nHAp was significantly higher than on the micro-fibers, although the adsorption per unit area was less on the nano-fibers due to the much higher surface area of nano-fibers. The authors concluded that a combination of a micro- and nano-fiber hierarchical scaffold could be more beneficial for tissue engineering applications than the individual scaffolds provided the amount of nano- fibers could be suitably optimized.

Park et al in 2011²⁵ fabricated porous polycaprolactone/hydroxyapatite (PCL/HA) blend scaffolds using a 3D plotting system for bone tissue engineering. The authors designed and fabricated three types of scaffolds: those from polycaprolactone (PCL), those from PCL and hydroxyapatite (HA), and those from PCL/HA and with a shifted pattern structure (PCL/HA/SP scaffold). Shifted pattern structure was fabricated to increase the cell attachment/adhesion. The PCL/ HA/SP scaffold had a lower compressive modulus than PCL and PCL/HA scaffold. MTT assay and alkaline phosphatase activity results for the PCL/HA/SP scaffolds were significantly enhanced compared to the results for the PCL and PCL/HA scaffolds. According to their degree of cell proliferation/differentiation, the scaffolds were in the following order: PCL/HA/SP> PCL/HA>PCL. The authors concluded that these 3D scaffolds will be applicable for tissue engineering based on unique plotting system.

Chen et al in 2010²⁶ Prepared Composite Electrospun Nanofibers of Polycaprolactone and Nanohydroxyapatite to produce 300 nm nanofibers containing 0 , 25, and 50 wt% of nHAP for Osteogenic Differentiation of Stem Cells. Nanocomposites of poly-caprolactone (PCL) and nanohydroxyapatite (nHAP) were

prepared by the composite nanofibers were characterized for structure, morphology, and mechanical properties. Mesenchymal stem cells grown on the nanofibers show different degree of osteogenic differentiation dependent on nHAP content with the highest nHAP content giving the best mineralization.

Kim JY et al in 2010²⁷ fabricated Solid free-form fabrication-based PCL/HA scaffolds for bone tissue engineering. The bone regeneration potential of the scaffolds was compared with that of PCL scaffolds fabricated with the same system. The fabricated scaffolds had a pore size of 400 μm and a porosity of 66.7%. The PCL/HA scaffolds had higher mechanical strength and modulus than the PCL scaffolds. To compare the osteogenic potential, the two types of scaffolds were seeded with rat osteoblasts and cultured in vitro or implanted subcutaneously into athymic mice. The cells cultured on PCL/HA scaffolds expressed higher levels of osteopontin and osteonectin, both of which are osteogenic proteins. The authors concluded that PCL/HA scaffolds resulted in larger bone area and calcium deposition in the implants compared to the PCL scaffolds.

Joshua R. Porter et al in 2009²⁸ fabricated Biodegradable poly(3-caprolactone) nanowires for bone tissue engineering applications. They found that Nanowire surfaces demonstrated enhanced MSC adhesion, proliferation, ALP activity, mineralization, osteocalcin, and osteopontin. Also they concluded that PCL nanowire surfaces encapsulated with HA, warrants the efficacy for 3D engineering of bone tissues.

Zhao et al in 2008²⁹ fabricated a porous composite scaffold composed of HA scaffold and polycaprolactone (PCL) by the method of polymer impregnating to

produce HA scaffold coated with PCL lining. Subsequently, the composite scaffolds were deposited with biomimetic coating for improving the bioactivity. The authors suggested that the HA/PCL composite scaffolds with improved mechanical property and bioactivity is expected to be a promising bone substitute in tissue engineering applications.

Venugopal et al in 2008³⁰ conducted a study to evaluate the effect of Nanobioengineered Electrospun Composite Nanofibers and Osteoblasts for Bone Regeneration using PCL and HA /Gel. Nanofibrous scaffolds were electrospun into a blend of synthetic biodegradable polycaprolactone (PCL) with hydroxyapatite (HA) and natural polymer gelatin (Gel) at a ratio of 1:1:2 (PCL/HA/Gel) compared to PCL (9%), PCL/HA (1:1), and PCL/Gel (1:2) nanofibers. The interconnecting porous structure of the nanofibrous scaffolds provides large surface area for cell attachment and sufficient space for nutrient transportation. The tensile property of composite nanofibrous scaffold (PCL/HA/Gel) was highly flexible and allows penetrating osteoblasts inside the scaffolds for bone tissue regeneration. The cell proliferation (88%), alkaline phosphatase activity (77%), and mineralization (66%) of osteoblasts were significantly ($P < 0.001$) increased in composite nanofibrous scaffold compared to PCL nanofibrous scaffolds. The study concluded electrospun PCL/ HA/Gel composite nanofibrous scaffolds has potential for the proliferation and mineralization of osteoblasts for bone regeneration.

Wutticharoenmongkol et al in 2007³¹ evaluated the Osteoblastic Phenotype Expression of MC3T3-E1 Cultured on Electrospun Polycaprolactone Fiber Mats Filled with Hydroxyapatite Nanoparticles and concluded that greatest extent of

mineralization was seen on the cells grown on the surface of PCL/Hap which is a desirable property for tissue engineering.

Kim et al in 2007³² fabricated Poly ϵ -caprolactone(PCL)/ hydroxyapatite (HA) composite scaffolds by particulate leaching and freeze drying routes with different HA content. Porosity was decreased with HA addition, while mean pore size was maintained at around porogen size regardless of HA content. Compressive modulus was increased with increasing HA content. In that study, the optimum content of HA was around 40% in weight against PCL to obtain the highest compressive modulus with keeping porosity above 85%. HA apparently enhanced proliferation of osteoblast-like MG63 cells in PCL/HA composite scaffolds. The authors concluded that typical adhesion, migration and aggregation procedure of MG63 cells were found on PCL, while spreading morphology only was found on HA even at the early stage of adhesion without migration or aggregation.

Hyun et al in 2007³³ fabricated and characterized poly ϵ -caprolactone(PCL) and hydroxyapatite(HA)by solvent casting and salt leaching method. The scaffolds have interconnected pore structure with pore size ranging from 10 μ m to 500 μ m. The pore size of PCL scaffold and PCL/HA scaffold were similar to that of the salt particles. The pore walls became thick and the small pores on the surface of macropores were formed as the HA increased. MTT assay showed that HA content did not affect initial cell attachment in both PCL scaffolds and PCL/HA scaffolds. The osteoblasts proliferated in both scaffolds, but the cell number was higher in the PCL/HA composite scaffolds. It was found that the incorporation of hydroxyapatite enhances bone cell proliferation rather than initial cell attachment in PCL/HA

composite scaffolds. The results suggested that the PCL/HA composite scaffolds have a potential for the bone tissue engineering applications

Wutticharoenmongkol P et al in 2006³⁴ conducted a study to evaluate the effect on hydroxyapatite loading on Fibrous PCL scaffolds by electrospinning technique and outcome of the study was so that Fibrous PCL scaffolds on loading with nano particles of HA/CaCO₃ resulted in increased diameter and tensile strength in a concentration dependent manner. Diameter of fibers was controlled by concentration of polymer solution and applied electric potential. The fibers showed no cyto-toxic effect on fibroblast cells[saos2].

Sanchavanakit N et al in 2006³⁵ prepared and characterized a Novel Bone Scaffolds Based on Electrospun Polycaprolactone Fibers Filled with Nanoparticles of hydroxyapatite. The potential for use of these e-spun fiber mats as bone scaffolds was assessed by mouse calvaria derived pre-osteoblastic cells, MC3T3-E1, in terms of attachment, proliferation, differentiation, and mineralization. Despite the lower number of cells attached at early time points, both the fibrous scaffolds supported the proliferation of MC3T3-E1 at similar levels to tissue-culture polystyrene plate (TCPS), with the cells growing on the PCL/ HAp fiber mat (i.e., PCL/HAp-FS) showing the greatest proliferation rate on day 3 after the initial attachment period of 16 hrs. The authors concluded that the scaffold made from electrospun PCL/HA composite fibers would be the best to promote bone-cell activities.

Myung-Seob Khil et al in 2004³⁶ fabricated a novel polycaprolactone Matrix Via Electrospinning for Tissue Engineering. Polycaprolactone (PCL) was dissolved in solvent mixtures of methylenechloride/*N*, *N*-dimethyl formamide with ratios of

100/0, 75/25, and 50/50 (v/v) for electrospinning. The filament was formed by coagulation of the spinning solution following the well-known principle of phase separation in polymer solutions valid in other wet shaping processes. To evaluate the feasibility of three-dimensional fabric as scaffold matrices, the plain weave, which is the simplest of the weaves and the most common, was prepared with porous PCL filament. The growth characteristics of MCF-7 mammary carcinoma cells in the woven fabrics showed the important role of matrix microstructure in proliferation. The authors concluded that the woven fabrics, consisting of porous filaments via electrospinning, may be suitable candidates as tissue engineering scaffolds.

PCL/BG COMPOSITE MEMBRANES

Fereshteh et al in 2015³⁷ evaluated Mechanical properties and drug release behavior of PCL/zein coated 45S5 bioactive glass scaffolds fabricated by foam replication method for bone tissue engineering application. the authors stated that by coating the BG scaffolds with PCL or PCL/zein blend the mechanical properties of the scaffolds were substantially improved, i.e., the compressive strength increased from 0.00470.001 MPa (uncoated BG scaffolds) to 0.1570.02 MPa (PCL/zein coated BG scaffolds). A dense bone-like apatite layer formed on the surface of PCL/zein coated scaffolds immersed for 14 days in simulated body fluid (SBF). The study concluded that the developed scaffolds exhibited attractive properties for application in bone tissue engineering research.

Yufeng Zhang et al in 2014³⁸ conducted a study aimed to achieve periodontal regeneration of strontium-incorporated mesoporous bioactive glass (Sr-MBG) scaffolds in an osteoporotic animal model carried out by bilateral ovariectomy (OVX). Periodontal fenestration defects treated with Sr-MBG scaffolds

showed greater new bone formation (46.67%) when compared to MBG scaffolds (39.33%) and control unfilled samples (17.50%). The number of TRAP (tartrate-resistant acid phosphatase)-positive osteoclasts was also significantly reduced in defects receiving Sr-MBG scaffolds. Thus the results suggest that Sr-MBG scaffolds can provide greater periodontal regeneration.

Samaneh Izadi et al in 2014³⁹ conducted a study to evaluate the nanostructure properties of bioactive glasses. In this research bioglass powder was synthesized with sol-gel method to achieve nanostructure powder. The glass powder was characterized with transmission electron microscope [TEM]. The SEM results show that nanopores and macropores are connectively distributed in whole part of scaffolds. The compressive strength of scaffolds was 0.8 MPa. Overall, the scaffold is suggested that is appropriate alternative for bone tissue engineering.

Mansoorah Otadi et al in 2014⁴⁰ conducted a study and in that study sol-gel derived glasses based on CaO-SrO-SiO₂-P₂O₅ system were prepared. The results showed that the substitution of Sr for Ca in the glass, increased the mechanical Strength of nanofibers. composition poly(ϵ -caprolactone)/bioglass were electrospun using a high DC voltage of 18 kV at a distance of 16cm. SEM morphology of the PCL/BG electrospun nanocomposite revealed that bioglass nanoparticles were distributed in nanofibers during the electrospinning process. The results revealed that BG contains a higher percentage of strontium oxide increases significantly ($p < 0.05$) the tensile strength of composite than other BGS.

Patrina S Poh et al in 2013⁴¹ fabricate and characterise bioactive composite scaffolds for bone tissue engineering applications. 45S5 Bioglass® (45S5) or strontium-

substituted bioactive glass (SrBG) were incorporated into polycaprolactone (PCL) and fabricated into 3D bioactive composite scaffolds utilising additive manufacturing technology. In vitro studies were conducted using MC3T3 cells under normal and osteogenic conditions. All scaffolds were shown to be non-cytotoxic, and supported cell attachment and proliferation.

Farnaz Naghizadeh et al in 2013⁴ fabricated a 3D scaffold using polycaprolactone (PCL) and silicate based bioactive glass-ceramic (R-SBgC). Different concentrations of R-SBgC prepared from rice husk ash (RHA) were combined with PCL to fabricate a composite scaffold using thermally induced phase separation (TIPS) method. The products were then characterized using SEM and EDX. The results demonstrated that R-SBgC in PCL matrix produced a bioactive material which has highly porous structure with interconnected porosities. The study concluded that, it is possible to fabricate a PCL/bioactive glass-ceramic composite from processed rice husk. Varying the R-SBgC concentrations can control the properties of this material, which is useful in the development of the ideal scaffold intended for use as a bone substitute in nonload bearing sites.

Radev et al in 2013⁴² evaluated In vitro Bioactivity of Polycaprolactone/Bioglass Composites. A series of Polycaprolactone and Bioglass systems were synthesized at different quantity of the organic/inorganic components. The 85S Bioglass was prepared via sol-gel method. It was added to the Polycaprolactone matrix at 20, 50 and 80 weight (wt.) %, respectively. In vitro bioactivity of the prepared composites was evaluated in 1.5 Simulated Body Fluid (1.5 SBF). The obtained composite materials before and after static in vitro test were characterized

by FTIR and SEM. The obtained experimental data proved that the synthesized composites exhibited good in vitro bioactivity.

Ji-Hoon Jo et al in 2009⁴³ compared In Vitro/In Vivo Biocompatibility and Mechanical Properties of Bioactive Glass Nanofiber and Poly(e-caprolactone) Composite Materials. In that study, a poly(e-caprolactone) (PCL)/bioactive glass (BG) nanocomposite was fabricated using BG nanofibers (BGNFs) and compared with an established composite fabricated using microscale BG particles. The biological and mechanical properties of the PCL/BGNF composites were evaluated and compared with those of PCL/BG powder (BGP). Because the PCL/BG composite containing 20 wt % BG showed the highest level of alkaline phosphatase (ALP) activity, all evaluations were performed at this concentration except for that of the ALP activity itself. In vitro cell tests using the MC3T3 cell line demonstrated the enhanced biocompatibility of the PCL/BGNF composite compared with the PCL/BGP composite. Furthermore, the PCL/BGNF composite showed a significantly higher level of bioactivity compared with the PCL/BGP composite. The results of the in vivo animal experiments using Sprague–Dawley albino rats revealed the good bone regeneration capability of the PCL/BGNF composite when implanted in a calvarial bone defectness of the PCL/BG composite was further increased when the BGNFs were incorporated. These results indicate that the PCL/BGNF composite has greater bioactivity and mechanical stability when compared with the PCL/BG composite and great potential as a bone tissue engineering material.

Oana Bretcanu et al in 2009⁴⁴ conducted a study to evaluate the effect of Electrospun nanofibrous biodegradable polyester coatings on Bioglass-based glass-

ceramics for tissue engineering and it was found that all samples are highly bioactive and promote hydroxyapatite crystal growth on their surfaces after 7 days of immersion in SBF. The authors concluded that these membranes with bioactivity is a promising bone substitute in tissue engineering applications.

Lee et al in 2008⁴⁵ evaluated Bioactivity improvement of poly(epsilon-caprolactone) membrane with the addition of nanofibrous bioactive glass. Nanofibrous glass with a bioactive composition was added to a degradable polymer poly(epsilon-caprolactone) (PCL) to produce a nanocomposite in thin membrane form (approximately 260 micron). The bioactivity and osteoblastic responses of the nanocomposite membrane were examined and compared with those of a pure PCL membrane. Glass nanofibers with diameters in the range of hundreds of nanometers were added to a PCL solution at 20 wt%, and the mixture was stirred vigorously and air dried. The obtained nanocomposite membrane showed that many chopped glass nanofibers formed by the mixing step were embedded uniformly into the PCL matrix. The nanocomposite membrane induced the rapid formation of apatite-like minerals on the surface when immersed in a simulated body fluid. Murine-derived osteoblastic cells (MC3T3-E1) grew actively over the nanocomposite membrane with cell viability significantly improved compared with those on the pure PCL membrane. Moreover, the osteoblastic activity, as assessed by the expression of alkaline phosphatase, was significantly higher on the nanocomposite membrane than on the pure PCL membrane. The study concluded that the developed nanocomposite of the bioactive glass-added PCL might find applications in the bone regeneration areas such as the guided bone regeneration (GBR) membrane.

MATERIALS & METHODS

The study protocol was approved by Institutional Research committee [Sree Mookambika Institute of Dental Sciences, Tamilnadu with Reference no-06/06/2015]. Laboratory facilities for the study was provided by the Biotechnology and Polymer wing of Sree Chitra Thirunal Institute for Medical Sciences and Technology, Trivandrum, India, for a period of 3 months.

MATERIALS

For Membrane fabrication

- Polycaprolactone polymer Pellets with M_{wt} 80,000(Sigma Aldrich Pt Ltd., USA). [CP-1]
- Bioactive glass powder [Biomaterial wing, Sree Chitra Thirunal Institute of Medical science and Technology] [CP-2]
- Nano Hydroxyapatite powder [Biomaterial wing , Sree Chitra Thirunal Institute of Medical science and Technology]
- Solvents- Dichloro methane and Dimethyl formamide (Sigma Aldrich Pt Ltd., USA) [CP-3a,3b]
- Electrospinning machine[Holmarc, USA]:- Polymer Technology wing, Sree Chitra Thirunal Institute of Medical science and Technology[CP-4]
- Elctronic weighing Machine[CP-5]
- Measuring cylinder 25 ml [Borosil][CP-6]
- Automatic Stirrer[CP-7]
- 10ml syringes with 21 gauge needle [BD Discardit, India] [CP-8]
- Vaccum oven[CP-9]

For analyzing Mechanical properties

- Specimen cutting dies [ISO standard 527-2 Type 5B] [CP-10a,b]
- Thickness Gauge[CP-11]
- Universal testing machine (Instron 3345, single column, UK)[CP-12]

For analyzing Morphology [Fiber Diameter and Pore Diameter, Fiber Distribution and Pore Distribution]

- Scanning Electron Microscope[Hitachi-model-S-2400, JEOL, JSM-6390, model 7582, Japan][CP-13]
- ImageJ software

For Chemical analysis[Presence of Functional group]

- FTIR spectrometer[CP-14]

For Thermal analysis

- Thermogravimetric analyzer[Shimadzu TGA-50 (Shimadzu Corporation, Kyoto, Japan)]-provided by Chemistry lab, Fine Arts College,Trivandrum[CP-15]

For Cytotoxicity assessment

- UV irradiator for sterilization of samples [Biogenix Research Centre, Trivandrum, India]
- L929 Mouse fibroblast cells[National Centre for Cell Science, Pune, India].
- Dulbecos Modified Eagles Medium [Biogenix Research Centre, Trivandrum, India]
- Phase contrast microscope(Olympus CKX41) for MTT assay observation provided by [Biogenix Research Centre, Trivandrum,India][CP-16]

- succinate dehydrogenase Enzyme[Biogenix Research Centre, Trivandrum,India]
- PBS with PH of 7.4[Polymer Technology wing, Sree Chitra Thirunal Institute of Medical science and Technology]
- Incubator[CP-17]
- Imaging software Optika vision-pro for Image capturing

Method of GTR Membrane Fabrication

Membranes were fabricated by Electrospinning technique using PCL[1 gm] and blending the PCL with different weight concentrations of Hydroxyapatite [HAP] and Bioactive glass[BG].The weight concentrations of both HAP and BG used was 2wt% [0.02gm], 5wt% [0.05gm],10wt% [0.1gm] and 15wt% [0.15gm].The initial step was weighing 1gm of PCL followed by weighing of filler either HAP or BG with appropriate wt% concentration ;i.e 2wt % of either HAP/BG is added to 1gm PCL and is transferred to a glass tube. Next step was addition of solvents i.e Dichloromethane and Dimethylformamide in the ratio of 8:2 ml respectively for dissolving the solutes. To this magnetic pellet was added which acts as a stirrer and placed over automatic stirring machine. After 3hrs of stirring, a clear homogenous solution was obtained.[CP-18]

Spinning was performed at predetermined conditions of 10% solution concentration, applied potential of 12 Kv with a feed rate of 1 ml/h. The desired solutions were loaded into a 10 ml syringe, the opening end of which was connected to a 21 gauge stainless steel needle that was used as the nozzle. A mandrel rotating at 500 rpm was used as the collector and was placed at a distance of 15 cm from the needle tip. A Gamma High-Voltage Research power supply was used to generate a high DC potential. A Scientific syringe pump was used to control the feed rate of the

polymer solution. The collection time for the above process was fixed about 10 hrs. In the process of electrospinning, when this high electrostatic voltage [12kv] is imposed on a drop of solution held by its surface tension at the end of a needle tip, leading to distortion of the liquid into a conical jet (known as the Taylor cone), ejecting fibres. Once the voltage exceeds a critical value, the electrostatic force overcomes the solution surface tension, and a stable liquid jet is ejected from the cone tip. The solvent evaporates as the jet travels through the air, leaving behind ultra-fine fibres with a high surface-to-volume ratio collected on an electrically-grounded target. After the process, the electrospun fibers in the form of sheet was obtained. [CP-19]

So total of 9 samples divided in to three groups was fabricated using the electrospinning technique i.e an electrospun sample of PCL alone which acts as control group, 4 samples of PCL blended with different concentrations of HA [1gm PCL with 0.02gmHA, 0.05gmHA, 0.1gmHA, 0.15gmHA] which is considered as a second group and 4 samples of 1gm PCL blended with different concentrations of BG [1gm PCL with 0.02gmBG, 0.05gmBG, 0.1gmBG, 0.15gmBG] as third group. All these nano fibrous sheets were dried in a vacuum oven at 40°C for about 48 h to remove the residual solvent.

Scanning Electron Microscopy (SEM) of Electrospun Membranes

The 3D morphology of the electrospun GTR membranes was observed by scanning electron microscopes (Hitachi-model-S-2400, JEOL, JSM-6390, model 7582, Japan). The samples were sputter coated with gold palladium and imaged in order to study the Fiber morphology. The average fiber diameter and pore diameter, were measured using Image J software.

Mechanical Characterization of Membranes

The static mechanical properties were determined with universal testing machine (Instron 3345, single column, UK) with the use of a 100 N load cell under a cross-head speed of 10 mm/min (Gauge length 20 mm) at ambient conditions. Dumbbell shaped specimens as per ISO standard ISO 527-2 Type 5B were used[CP-20]. At least 5 set of specimens were tested for each type of electrospun fibrous GTR membranes to evaluate Tensile strength, Youngs modulus and Elongation at break.[CP-21]

Membrane thickness

Average thickness was measured using Thickness Gauge[CP-22]. The average thickness of the membranes at five random positions was adopted as the mean thickness of the membrane

In-Vitro Hydrolytic Degradation Studies

In-vitro hydrolytic degradation behavior of GTR Membranes in PBS at 37⁰C was monitored by observing the changes in weight, morphology and mechanical properties of membranes after different time period [14 days and 28 days]. For weight loss studies, circular samples with 20mm diameter were incubated in a closed bottle containing 30mL phosphate buffer solution (PBS) having pH 7.4 at 37 ⁰C [CP-23,24]. The initial weight (Wi) of the membrane before incubating in PBS was measured and the membranes were retrieved after 28 days. The retrieved membranes were washed with deionized water, dried in a vaccum oven and weighed (Wf) until constant weight is attained. The percentage weight loss was estimated using the equation

$$\text{Gravimetric weight loss (\%)} = (W_i - W_f) / W_i \times 100$$

For mechanical property evaluation, dumbbell specimens as per ISO standard ISO 527-2 Type 5B were used and the mechanical performance of the membranes after incubating in PBS (pH 7.4) at 37 °C for different time period [14 days and 28 days] was evaluated using universal testing machine (Instron 3345, single column, UK).

Chemical characterization of scaffolds using FTIR

The presence of nHAP and BG on PCL fibers was analyzed using ATR-FTIR.

Thermal analysis

Thermogravimetric analysis (TGA) was completed with a Shimadzu TGA-50 (Shimadzu Corporation, Kyoto, Japan). Samples were placed in the balance system and heated from room temperature to 900 °C at a heating rate of 10°C min⁻¹ under a nitrogen atmosphere.

Determination of cytotoxicity

Cell culture

For biological evaluation, L929 mouse fibroblast cells were procured from the National Centre for Cell Science, Pune, India. The cells were grown in DMEM supplemented with 10% FBS and containing the antibiotics penicillin, streptomycin and amphotericin B (5000 units) in a humidified incubator at 5%CO₂ at 37±0.2°C. The cells were regularly monitored by phase contrast inverted light microscopy. The medium was changed once in three days. The confluent monolayer was sub-cultured and maintained for further studies.

Sample preparation

Samples were treated with 70 % ethanol for 10 minutes followed by UV irradiation for 30 minutes and incubated in serum free media for 24 hours in a humidified incubator at 5%CO₂ at 37 ± 0.2⁰C.

Evaluation of the toxicity of material extracts by MTT assay

The cytotoxicity of materials extracts was evaluated as per ISO10993-5 on L-929 mouse fibroblast cell culture. The extract of the material was prepared with DMEM medium by incubating for 48h. The above medium was used to grow L929 cells for 24 hours under standard conditions. The percentage of the surviving fibroblast cells were quantified by the MTT assay and the morphological changes of the cells were monitored by phase contrast microscopy.

MTT assay is carried out to measure mitochondrial cellular metabolism (viability) and number of viable cells. MTT assay is based on the capability of metabolically active fibroblast cells to reduce the yellow water-soluble tetrazolium salt (MTT) to purple formazan crystals using the mitochondrial enzyme succinate dehydrogenase (SDH). The intensity of purple colour so formed is proportional to the number of viable cells. Following the experiment the culture was washed with 1 x PBS and then 200 µl MTT solution per ml culture (MTT 5 mg/ml dissolved in PBS and filtered through a 0.2 µm filter before use) were added. The whole content was again incubated at 37⁰C for 3h and 300 µl DMSO were added to each culture well. The whole content was incubated at room temperature for 30 min until all cells were lysed and a homogenous colour was obtained. The solution was centrifuged for 2 min to sediment cell debris. The optical density (OD) was measured spectro-

photometrically at 540 nm. Cells treated with MTT solution without sample was used as control. The % viability was calculated as follows.

$$\% \text{ Viability} = \frac{\text{OD of test}}{\text{OD of control}} \times 100$$

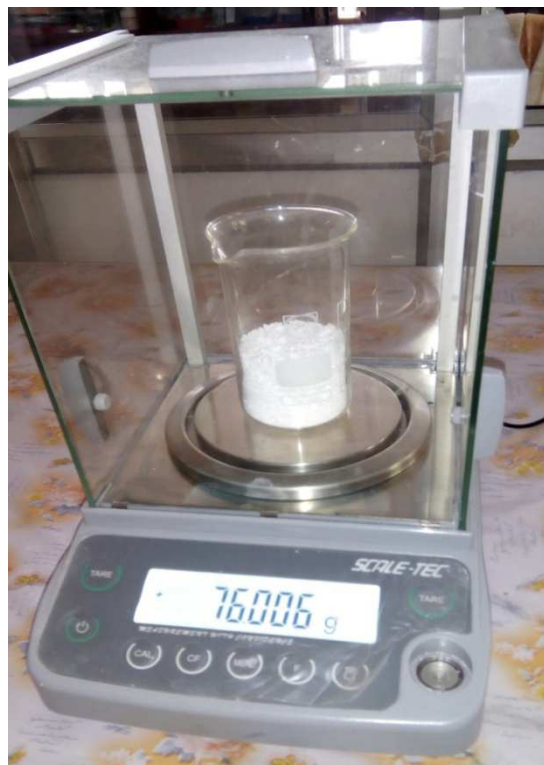
Direct contact method

The cytotoxicity of materials under the direct contact of cell was determined by direct contact assay. L929 fibroblast cells (1×10^4 cells/m) were seeded on to a 24 well plate (BD Falcon) and allowed to proliferate for 24 h to form a sub-confluent layer. Then the material (1 cm diameter) was placed over the monolayer and allowed to proliferate for 24 h in a CO₂ incubator. After the incubation, cells were evaluated for changes in morphology with respect to a control (cells grown without materials) under inverted phase contrast microscope (Olympus CKX41) attached with an imaging camera. The images were captured using imaging software Optika vision-pro.

COLOR PLATES



CP-1: Polycaprolactone polymer Pellets



CP2- Bioactive glass powder



Cp3a-Dichloromethane



CP-3b-dimethyl formamide



Syringe pump



Rotating Mandrel

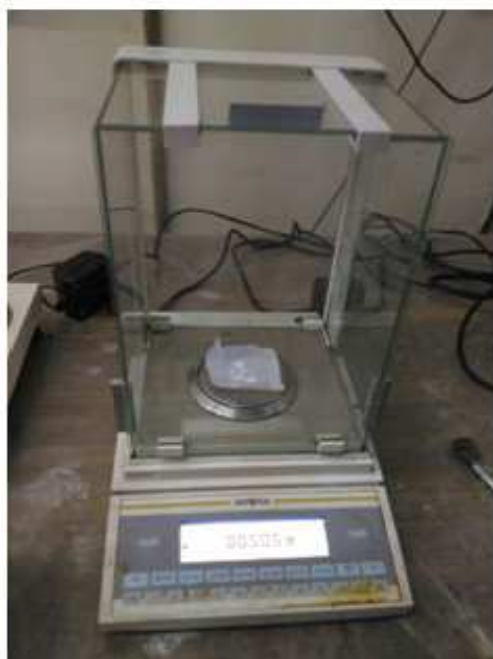


Woven sheets in rotating mandrel



Power supply

Cp- 4 Electrospinning setup



Cp-5: Electronic weighing machine



Cp-6: Measuring cylinder 25 ml



Cp-7: Automatic Stirrer



Cp-8: 10ml syringes with 21 gauge needle



Cp-9:Vaccum oven



CP-10a, 10b: Specimen Cutting Dies



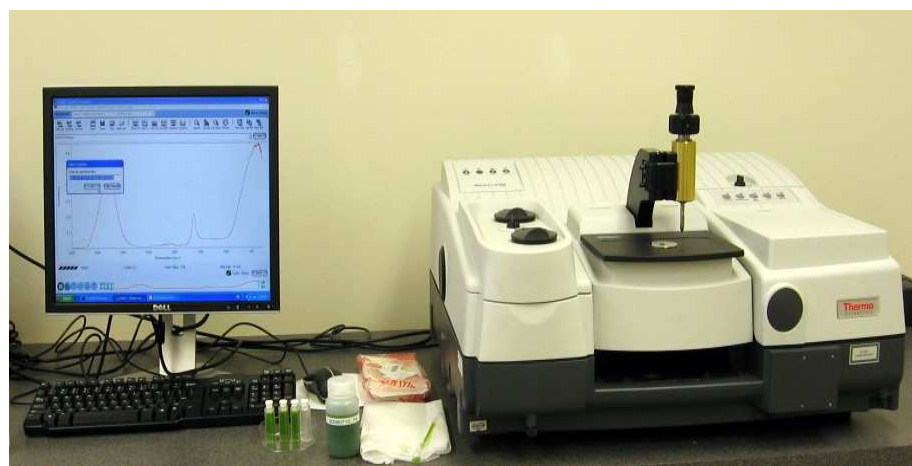
CP-11: Thickness Gauge



CP-12: Universal testing machine (Instron 3345, single column, UK)



CP-13: Scanning Electron Microscope[Hitachi-model-S-2400, JEOL, JSM-6390, model 7582, Japan][CP-13]



CP-14:FTIR spectrometer



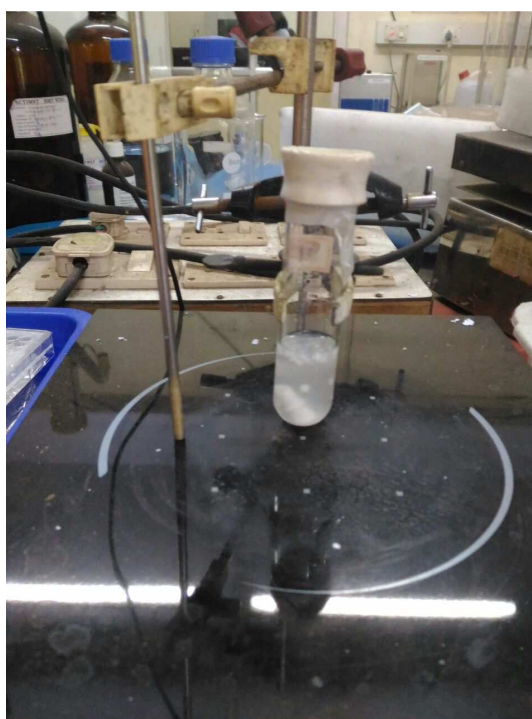
CP-15: Thermogravimetric analyzer[Shimadzu TGA-50 (Shimadzu Corporation, Kyoto, Japan)]



CP-16: Phase contrast microscope(Olympus CKX41)



CP-17- Incubator



CP-18:clear homogenous solution of Polymer and Bioactive Material



CP-19:Electrospun Nanofibrous sheets

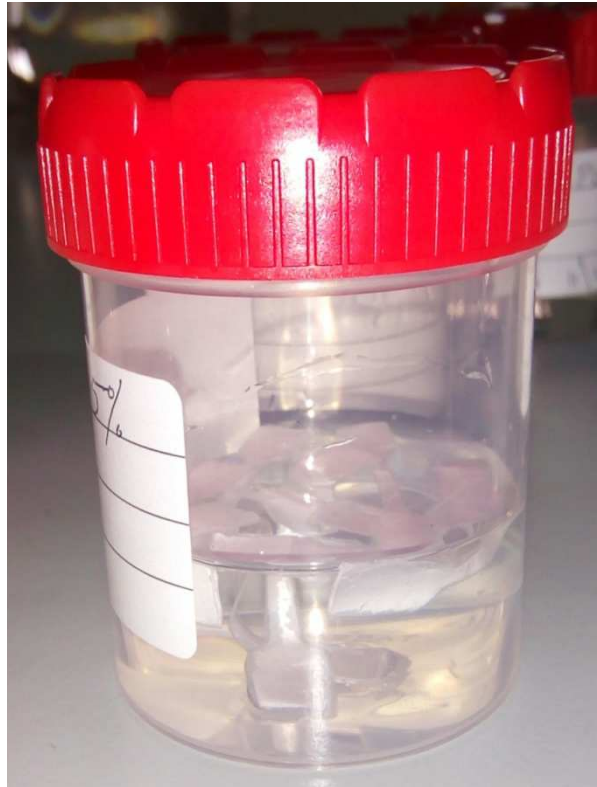


Cp-20-Dumbbell shaped specimen



CP-21-Measuring Mechanical Properties





Cp-23-Samples immersed in PBS



Cp-24-Samples placed in Incubator

RESULTS & OBSERVATIONS

Statistical analysis: The data was analyzed by Statistical Package for Social Sciences (SPSS 16.0) version. The data was tested for normality. One way ANOVA (Post hoc) followed by Dunnet t test applied to find statistical significant between the groups. Chi square test applied to find the statistical significance within the groups. P value less than 0.05 considered statically significant at 95% confidence interval.

Table-1: Comparison of Mean Fiber diameter between the groups

Groups	Fiber diameter [μm](MEAN \pm SD)	Compared with	p value
PCL	1.62 \pm 0.40	Different weight percentages of PCL -BG AND PCL- HA	0.02
PCL+BG2%	1.08 \pm 0.16	PCL+HA10%,15%	0.03
PCL+BG5%	0.99 \pm 0.24	PCL+HA15%	0.03
PCL+BG10%	0.91 \pm 0.23	PCL+HA15%	0.03
PCL+BG15%	0.90 \pm 0.21	PCL+HA15%	0.03
PCL+HA2%	0.95 \pm 0.22	PCL+HA15%	0.03
PCL+HA5%	0.97 \pm 0.33	PCL+HA15%	0.03
PCL+HA10%	0.89 \pm 0.26	PCL+HA15%	0.04
PCL+HA15%	0.49 \pm 0.58		

(p<0.05 considered statistically significant compared between the groups)

Table shows comparison of mean fiber diameter between the groups. From this table it is evident that PCL membrane showed higher fiber diameter [1.62 \pm 0.40] when compared with the fiber diameters of other membranes and was statistically significant. Among the PCL +BG group of membranes, PCL+BG2% [1.08 \pm 0.16] showed higher fiber diameter. Among the PCL+HA group of membranes,

PCL+HA2% showed higher fiber diameter. Overall there was decrease in fiber diameter with increasing different weight concentrations of filler particles.

Table-2: Comparison of Mean Pore diameter between the groups

Groups	Pore diameter[μm] (MEAN \pm SD)	Compared with	p value
PCL	2.51 \pm 0.80	PCL+HA15%	0.04
PCL+BG2%	2.45 \pm 0.92	PCL+HA15%	0.04
PCL+BG5%	2.36 \pm 1.19	PCL+HA15%	0.04
PCL+BG10%	2.22 \pm 0.79	PCL+HA15%	0.05
PCL+BG15%	2.11 \pm 0.60	PCL+HA15%	0.05
PCL+HA2%	2.24 \pm 0.82	PCL+HA15%	0.05
PCL+HA5%	2.32 \pm 0.70	PCL+HA15%	0.04
PCL+HA10%	2.00 \pm 0.72	PCL+HA15%	1.78
PCL+HA15%	1.90 \pm 0.67		

($p < 0.05$ considered statistically significant compared between the groups)

Table shows the comparison of mean pore diameter between the groups. Statistically significant higher pore diameter was exhibited by the PCL membrane[2.51 \pm 0.80 μm]when compared with PCL+HA15%[1.90 \pm 0.67] .significant difference in pore diameter was shown by all the membranes only when compared with PCL+HA15%.Overall there was decrease in pore diameter with increasing weight concentrations of filler particles.

**SEM IMAGES OF FABRICATED GTR MEMBRANES WITH
DIFFERENT MAGNIFICATIONS**

PCL

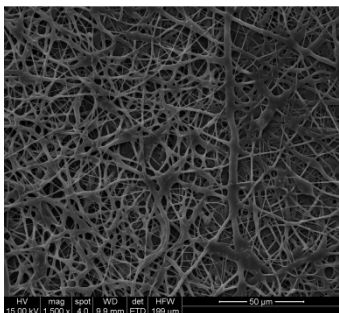


Image 01

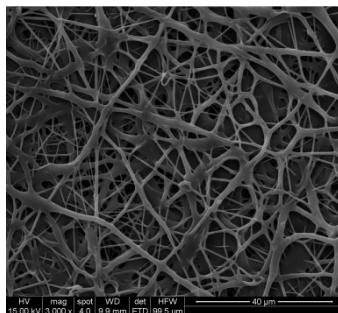


Image 02

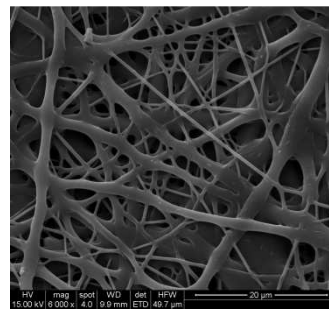


Image 03

PCL + BG2%

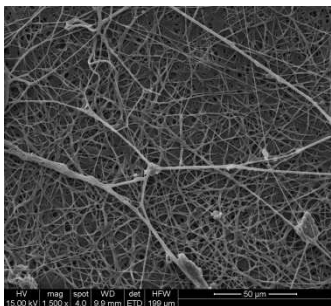


Image 04

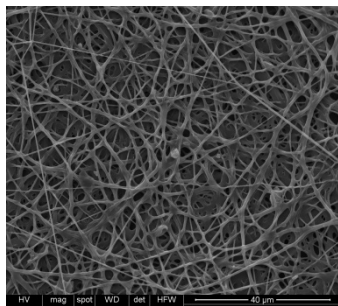


Image 05

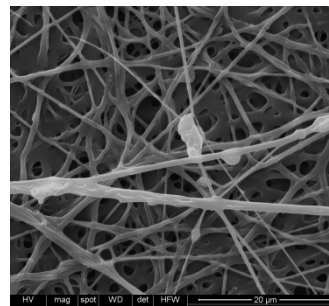


Image 06

PCL + BG5%

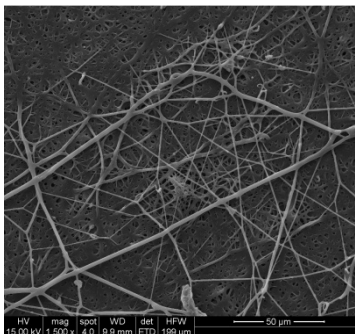


Image 07

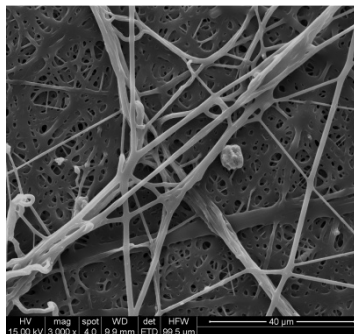


Image 08

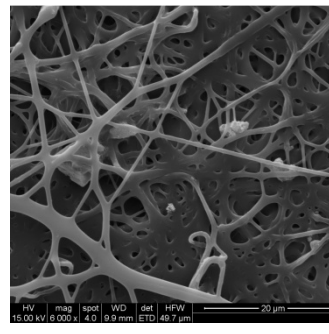


Image 09

PCL + BG10%

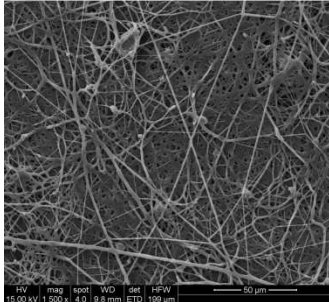


Image 10

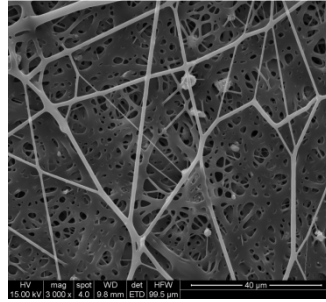


Image 11

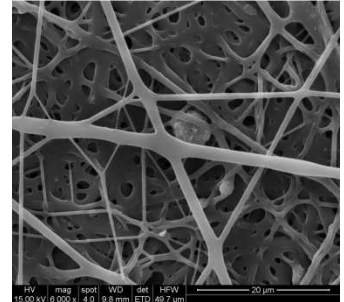


Image 12

PCL + BG15%

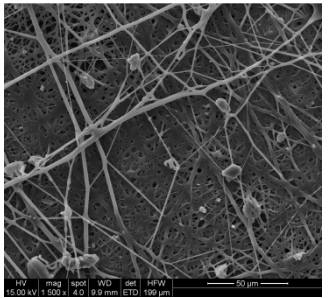


Image 13

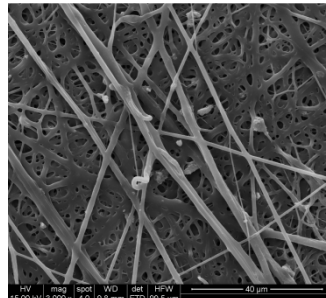


Image 14

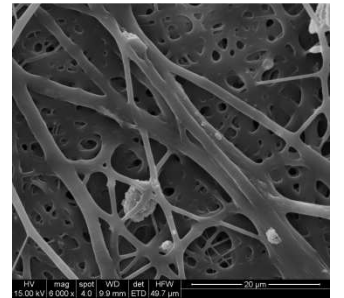


Image 15

PCL + HA2%

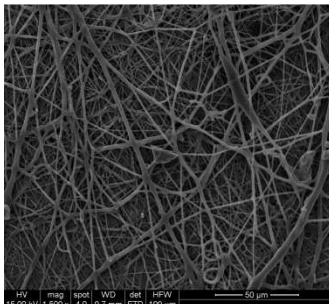


Image 16

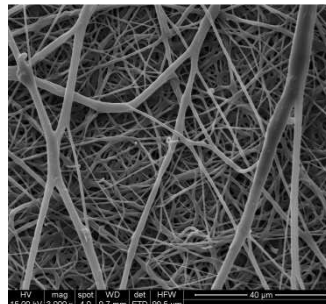


Image 17

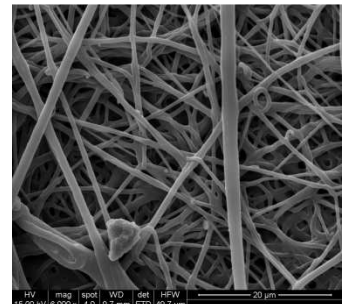


Image 18

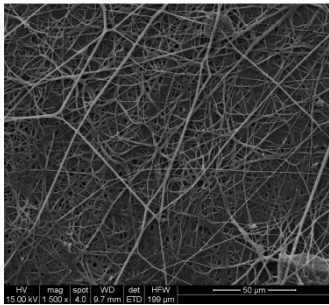


Image 19

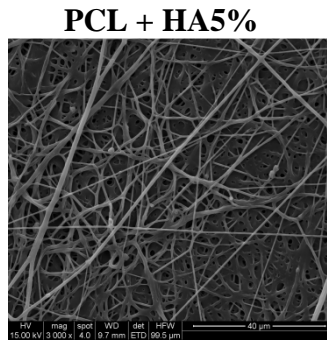


Image 20

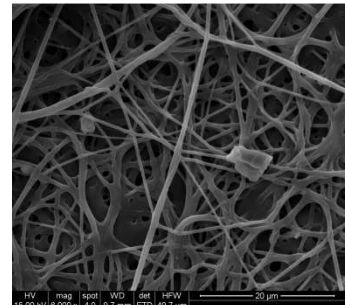


Image 21

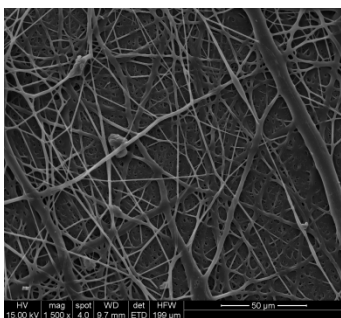


Image 22

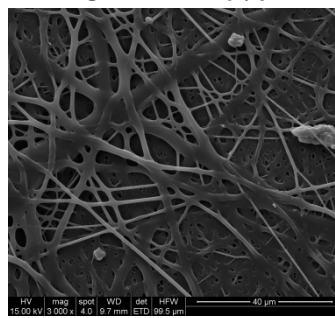


Image 23

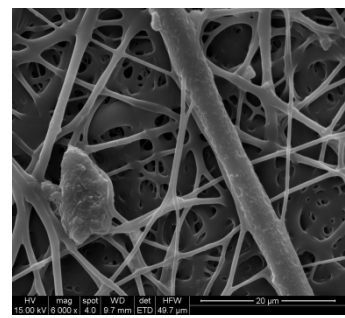


Image 24

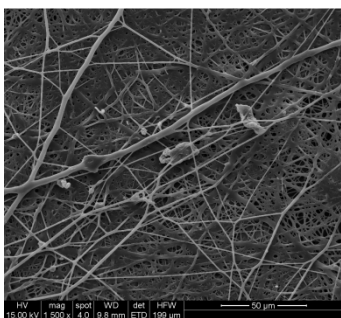


Image 25

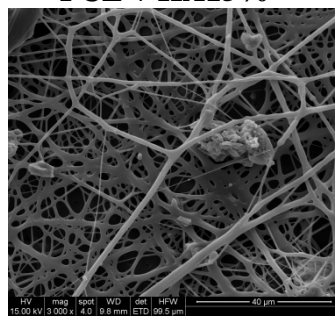


Image 26

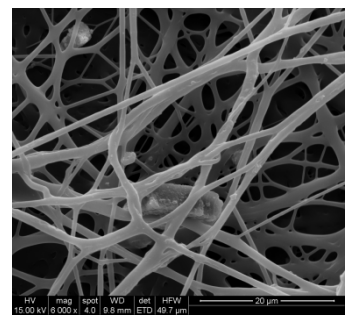


Image 27

Table-3: Comparison of Initial Mean Tensile Strength between the groups

Groups	Tensile strength [MPa] (MEAN±SD)	Compared with	p value
PCL	6.50±0.38	Different weight percentages of PCL -BG AND PCL- HA	0.001
PCL+BG2%	15.35±1.91	[PCL+BG10%,BG15%], [PCL+HA2%,5%,10%,15%]	0.04
PCL+BG5%	15.35±0.89	PCL+BG10%,15%], [PCL+HA2%,10%,15%]	0.04
PCL+BG10%	13.00±0.01	[PCL+BG15%], [PCL+HA2%,10%,15%]	0.04
PCL+BG15%	11.10±3.54	PCL+HA2%,10%,15%	0.03
PCL+HA2%	17.22±2.80	PCL+HA5%,10%,15%	0.03
PCL+HA5%	12.86±0.65	PCL+HA10%,15%	0.04
PCL+HA10%	10.42±0.21	PCL+HA15%	0.04
PCL+HA15%	9.55±1.04		

(p<0.05 considered statistically significant compared between the groups)

Table shows the mean values of initial tensile strength between the groups. From this table it is evident that Membrane made of PCL alone showed the least tensile strength [6.50±0.38MPa] when compared with the other membranes and was statistically significant. Among the composite membrane groups, PCL+HA2% [17.22±2.80MPa] showed the higher Tensile strength and least tensile strength for PCL+HA15% [9.55±1.04MPa]. Within the PCL+BG group, PCL+BG2% [15.35±1.91MPa] and PCL+BG15% [11.10±3.54MPa] showed the higher and lower tensile strength respectively.

Table-4: Comparison of Mean Tensile strength between the groups at 14 days

Groups	Tensile strength [MPa] (MEAN±SD)	Compared with	p value
PCL	6.40±0.07	Different weight percentages of PCL -BG AND PCL- HA	0.001
PCL+BG2%	15.14±0.99	[PCL+BG10%,15%],[PCL+HA2%,5%,10%,15%]	0.03
PCL+BG5%	14.92±1.60	[PCL+BG15%], [PCL+HA2%,5%,10%,15%]	0.04
PCL+BG10%	13.00±5.05	[PCL+BG10%,15%], [PCL+HA2%,10%,15%]	0.04
PCL+BG15%	10.56±2.42	PCL+HA2%,5%,15%	0.04
PCL+HA2%	16.46±0.12	PCL+HA5%,10%,15%	0.03
PCL+HA5%	12.55±0.75	PCL+HA10%,15%	0.04
PCL+HA10%	10.34±1.28	PCL+HA15%	0.05
PCL+HA15%	9.39±1.48		

(p<0.05 considered statistically significant compared between the groups)

Table shows the mean values of tensile strength between the groups after 14 days of degradation in PBS. Membrane made of PCL alone showed the least tensile strength [6.40±0.07MPa] when compared with the other membranes and was statistically significant. Among the composite membrane groups, PCL+HA2% [16.46±0.12MPa] showed the higher Tensile strength and least tensile strength for PCL+HA15% [9.39±1.48MPa]. Within the PCL+BG group, PCL+BG2% [15.14±0.99MPa] and PCL+BG15% [10.56±2.42MPa] showed the higher and lower tensile strength respectively. Overall there was reduction in initial tensile strength after 14 days of degradation which was found to be statistically significant.

Table-5: Comparison of Mean Tensile strength between the groups after 28 days

Groups	Tensile strength [MPa] (MEAN±SD)	Compared with	p value
PCL	5.67±0.58	Different weight percentages of PCL -BG AND PCL- HA	0.001
PCL+BG2%	14.30±4.68	[PCL+BG10%,15%], [PCL+HA5%,10%,15%]	0.03
PCL+BG5%	14.07±1.00	PCL+BG10%,15%, [PCL+HA5%,10%,15%]	0.04
PCL+BG10%	12.37±2.82	[PCL+BG15%], [PCL+HA2%,10%,15%]	0.03
PCL+BG15%	9.99±4.58	PCL+HA2%,5%,15%	0.03
PCL+HA2%	15.28±1.88	PCL+HA5%,10%,15%	0.01
PCL+HA5%	11.03±5.17	PCL+HA10%,15%	0.03
PCL+HA10%	9.83±3.84	PCL+HA15%	0.04
PCL+HA15%	8.75±2.89		

(p<0.05 considered statistically significant compared between the groups)

Table shows the mean values of tensile strength between the groups after 28 days of degradation in PBS. Membrane made of PCL alone showed the least tensile strength [5.67±0.58MPa] when compared with the other membranes and was statistically significant. Among the composite membrane groups, PCL+HA2% [15.28±1.88MPa] showed the higher Tensile strength and least tensile strength for PCL+ HA15% [8.75±2.89MPa]. Within the PCL+BG group, PCL +BG2% [14.30±4.68MPa] and PCL+BG15% [9.99±4.58MPa] showed the higher and lower tensile strength respectively. Overall there was statistically significant reduction in initial tensile strength after 28 days of degradation for all the membranes

Table-6: Comparison of Mean Tensile strength within the groups at different time periods

Groups	Tensile strength at initial (MEAN±SD) [MPa]	Tensile strength at 14 days (MEAN±SD) [MPa]	Tensile strength at 28 days (MEAN±SD) [MPa]	p value
PCL	6.50±0.38	6.40±0.07	5.67±0.58*	0.04
PCL+BG2%	15.35±1.91	15.14±0.99	14.30±4.68*	0.03
PCL+BG5%	15.35±0.89	14.92±1.60	14.07±1.00*	0.04
PCL+BG10%	13.00±0.01	13.00±5.05	12.37±2.82*	0.03
PCL+BG15%	11.10±3.54	10.56±2.42	9.99±4.58*	0.03
PCL+HA2%	17.22±2.80	16.46±0.12	15.28±1.88*	0.01
PCL+HA5%	12.86±0.65	12.55±0.75	11.03±5.17*	0.03
PCL+HA10%	10.42±0.21	10.34±1.28	9.83±3.84*	0.04
PCL+HA15%	9.55±1.04	9.39±1.48	8.75±2.89*	0.04

(*p<0.05 significant compared tensile strength at initial with 28 days)

Table shows the comparison of mean tensile strength at different time periods that is Initial, after 14 and 28 days. On comparing the initial Tensile strength with that of tensile strength at 28 days, all the membranes exhibited statistically significant reduction. Among the composite membranes PCL+HA2% higher significance [p value<0.01]. overall it is evident that tensile strength decreases with the increase in different weight concentrations of filler particles.

Table-7: Comparison of Initial Mean Youngs modulus between the groups

Groups	Youngs modulus [MPa] (MEAN±SD)	Compared with	p value
PCL	28.01±5.98	[PCL+BG2%,5%,10%],[PCL+HA2%,5%]	0.02
PCL+BG2%	55.46±8.06	[PCL+BG10%,15%],[PCL+HA2%,5%,10%,15%]	0.01
PCL+BG5%	53.28±6.76	[PCL+BG15%], [PCL+HA2%,5%,10%,15%]	0.04
PCL+BG10%	51.34±8.69	[PCL+BG15%], [PCL+HA2%,5%,10%,15%]	0.03
PCL+BG15%	31.74±1.48	PCL+HA2%,5%	0.03
PCL+HA2%	57.16±7.39	PCL+HA5%,10%,15%	0.02
PCL+HA5%	37.70±2.53	PCL+HA10%,15%	0.04
PCL+HA10%	31.13±2.03	PCL+HA15%	1.56
PCL+HA15%	31.07±3.39		

(p<0.05 considered statistically significant compared between the groups)

Table shows comparison of Initial mean Youngs modulus between the groups. Among the membranes, PCL exhibited the least youngs modulus[28.01±5.98MPa] when compared with [PCL+BG2%, 5%,10%], [PCL+HA2%, 5%]. Among the composite membranes, highest youngs modulus was observed with PCL+HA2%[56.29±7.84MPa] and was statistically significant on comparing with PCL+HA5%,10%,15%.

Table-8: Comparison of Mean Youngs modulus between the groups at 14 days

Groups	Youngs modulus [MPa] (MEAN±SD)	Compared with	p value
PCL	27.07±2.13	Different weight percentages of PCL -BG AND PCL- HA	0.02
PCL+BG2%	54.22±8.61	[PCL+BG10%,15%], [PCL+HA2%,5%,10%,15%]	0.03
PCL+BG5%	53.10±0.92	[PCL+BG15%], [PCL+HA2%,5%,10%,15%]	0.02
PCL+BG10%	51.29±0.87	[PCL+BG15%], [PCL+HA2%,5%,10%,15%]	0.02
PCL+BG15%	31.26±1.20	PCL+HA2%,5%	0.02
PCL+HA2%	56.29±7.84	PCL+HA5%,10%,15%	0.01
PCL+HA5%	37.54±0.88	PCL+HA10%,15%	0.04
PCL+HA10%	31.07±0.99	PCL+HA15%	1.75
PCL+HA15%	31.06±1.40		

(p<0.05 considered statistically significant compared between the groups)

Table shows comparison of mean Youngs modulus between the groups after 14 days of degradation in PBS. Among the membranes, PCL exhibited the least youngs modulus [27.07±2.13MPa] when compared with Different weight percentages of PCL -BG AND PCL- HA .Among the composite membranes, highest youngs modulus was observed with PCL+HA2% and was statistically significant on comparing with [PCL+HA5%,10%,15%].Among the PCL+BG group of composite membranes,highest youngs modulus was observed with PCL+BG2% and was statistically significant on comparing with [PCL+BG10%,15%], [PCL+HA2%,5%,10%,15%].

Table-9: Comparison of Mean Youngs modulus between the groups after 28 days

Groups	Youngs modulus [MPa] (MEAN±SD)	Compared with	p value
PCL	26.07±2.08	Different weight percentages of PCL -BG AND PCL- HA	0.02
PCL+BG2%	53.18±14.25	[PCL+BG10%,15%], [PCL+HA2%,5%,10%,15%]	0.03
PCL+BG5%	52.81±8.43	[PCL+BG10%,15%], [PCL+ HA2%,5%,10%,15%]	0.04
PCL+BG10%	50.87±15.46	[PCL+BG15%],[PCL+ HA2%,5%,10%,15%]	0.03
PCL+BG15%	31.05±10.03	PCL+HA2%,5%	0.04
PCL+HA2%	55.72±11.16	PCL+HA5,10%,15%	0.02
PCL+HA5%	36.94±12.36	PCL+HA10%,15%	0.04
PCL+HA10%	30.96±1.98	PCL+HA15%	1.45
PCL+HA15%	30.30±17.64		

(p<0.05 considered statistically significant compared between the groups)

Table shows comparison of mean Youngs modulus between the groups after Youngs modulus [26.07±2.08MPa] when compared with Different weight percentages of PCL -BG AND PCL- HA. Among the composite membranes, highest Youngs modulus was observed with PCL+HA2% [55.72±11.16]and was statistically significant on comparing with [PCL+HA5%,10%,15%].Among the PCL+BG group of composite membranes, highest Youngs modulus was observed with PCL+BG2 [53.18±14.25MPa] and was statistically significant on comparing with [PCL+BG10%,15%],[PCL+HA2%,5%,10%,15%].

Table-10: Comparison of Mean Youngs modulus within the groups at different time periods

Groups	Youngs modulus at initial [MPa] (MEAN±SD)	Youngs modulus after 14 days [MPa] (MEAN±SD)	Youngs modulus after 28 days [MPa] (MEAN±SD)	p value
PCL	28.01±5.98	27.07±2.13	26.07±2.08	1.89
PCL+BG2%	55.46±8.06	54.22±8.61	53.18±14.25*	0.04
PCL+BG5%	53.28±6.76	53.10±0.92	52.81±8.43	1.7
PCL+BG10%	51.34±8.69	51.29±0.87	50.87±15.46	1.45
PCL+BG15%	31.74±1.48	31.26±1.20	31.05±10.03	1.34
PCL+HA2%	57.16±7.39	56.29±7.84	55.72±11.16*	0.04
PCL+HA5%	37.70±2.53	37.54±0.88	36.94±12.36	1.45
PCL+HA10%	31.13±2.03	31.07±0.99	30.96±1.98	1.84
PCL+HA15%	31.07±3.39	31.06±1.40	30.30±17.64	1.56

(*p<0.05 considered statistically significant compared initial with 28 days)

Table shows Comparison of Mean Youngs modulus within the groups at different time periods .All of the membranes showed reduction in Youngs modulus when comparing the initial with Youngs modulus after 28 days of degradation. But statistical significant degradation was observed only in PCL+BG2% membrane i.e. from 55.46±8.06MPa to 53.18±14.25MPa [P value <0.05].

Table-11: Comparison of Initial Mean Elongation at break between the groups

Groups	Elongation at break[%] (MEAN±SD)	Compared with	p value
PCL	259.25±6.95	Different weight percentages of PCL -BG AND PCL- HA	0.001
PCL+BG2%	153.08±10.66	[PCL +BG5,10,15] AND [PCL+HA2%,5%,10%,15%]	0.003
PCL+BG5%	167.00±18.09	[PCL +BG10%,15%] AND [PCL+HA2%,5%,10%,15%]	0.004
PCL+BG10%	171.94±27.83	[PCL +BG15%] AND [PCL+HA2%,5%,10%,15%]	0.04
PCL+BG15%	182.74±35.30	PCL+HA 2%,5%,10%,15%	0.001
PCL+HA2%	127.80±7.38	PCL+HA5%,10%,15%	0.001
PCL+HA5%	179.30±23.43	PCL+HA10%,15%	0.001
PCL+HA10%	207.33±26.48	PCL+HA15%	0.04
PCL+HA15%	211.34±50.00		

(p<0.05 considered statistically significant compared between the groups)

Table shows the comparison of mean values of Initial Elongation at Break between the groups. Among the different groups, PCL membrane showed highest elongation at break when compared with other groups and was statistically significant. In composite membranes, PCL+HA15% showed higher elongation at break and least elongation at break for PCL+HA2%. There was statistically significant difference between the elongation at break of PCL+HA15% AND PCL+HA2%. Among the PCL+BG group PCL+BG15% had higher elongation at break and showed statistically significant difference with PCL+BG2% which exhibited the least percentage elongation. Overall there was increase in elongation at break with increasing the weight concentrations of filler particles in composite membranes.

Table-12: Comparison of Mean Elongation at break between the groups after 14 days

Groups	Elongation at break[%] (MEAN±SD)	Compared with	p value
PCL	258.00±67.08	Different weight percentages of PCL -BG AND PCL- HA	0.001
PCL+BG2%	152.86±10.52	[PCL +BG5%,10%,15%] AND [PCL+HA2%,5%,10%,15%]	0.004
PCL+BG5%	166.63±17.38	[PCL +BG10%,15%] AND [PCL+HA2%,5%,10%,15%]	0.003
PCL+BG10%	171.14±27.83	PCL +BG15% AND [PCL+HA2%,5%,10%,15%]	0.03
PCL+BG15%	182.21±20.07	[PCL+HA 2%,5%,10%,15%]	0.001
PCL+HA2%	127.60±8.48	[PCL+HA5%,10%,15%]	0.001
PCL+HA5%	178.49±22.33	PCL+HA10%,15%	0.001
PCL+HA10%	207.33±31.27	PCL+HA15%	0.001
PCL+HA15%	211.12±85.70		

(p<0.05 considered statistically significant compared between the groups)

Table shows the comparison of mean values of Elongation at Break between the groups after 14 days of degradation in PBS. From this table it is evident that after 14 days of degradation there was significant reduction in elongation in all the groups. Among the groups, higher elongation at break after 14 days was exhibited by PCL membrane and the least for PCL+HA2%. Among the PCL+BG composite membranes, PCL+BG15% had higher elongation and least for PCL+BG2% and was statistically significant. In PCL+HA composite membrane group, PCL+HA15% showed higher elongation at break.

Table-13: Comparison of Mean Elongation at break between the groups after 28 days

Groups	Elongation at break [%] (MEAN±SD)	Compared with	p value
PCL	257.12±62.86	Different weight percentages of PCL -BG AND PCL- HA	0.001
PCL+BG2%	152.35±4.78	[PCL +BG5%,10%,15%] AND [PCL+HA2%,5%,10%,15%]	0.004
PCL+BG5%	163.91±14.85	[PCL +BG10%,15%] AND [PCL+HA2%,5%,10%,15%]	0.003
PCL+BG10%	170.96±74.81	PCL +BG15% AND [PCL+HA2%,5%,10%,15%]	0.03
PCL+BG15%	181.30±1.44	[PCL+HA 2%,5%,10%,15%]	0.001
PCL+HA2%	126.82±10.54	[PCL+HA5%,10%,15%]	0.001
PCL+HA5%	178.22±10.02	PCL+HA10%,15%	0.001
PCL+HA10%	206.72±33.35	PCL+HA15%	0.001
PCL+HA15%	210.83±26.05		

(p<0.05 considered statistically significant compared between the groups)

Table shows the comparison of mean values of Elongation at Break between the groups after 28 days of degradation in PBS. After 28 days, PCL membrane showed higher Elongation at break when compared with other groups and was statistically significant. Among the PCL+BG group,PCL+BG15% showed higher elongation at break and among the PCL+HA group PCL+HA15% showed higher elongation at break.

Table-14: Comparison of Mean Elongation at break within the groups at different time periods

Groups	Initial Elongation at break [%](MEAN±SD)	Elongation at break after 14 days [%] (MEAN±SD)	Elongation at break after 28 days [%] (MEAN±SD)	p value
PCL	259.25±6.95	258.00±67.08	257.12±62.86*	0.05
PCL+BG2%	153.08±10.66	152.86±10.52	152.35±4.78	1.56
PCL+BG5%	167.00±18.09	166.63±17.38	163.91±14.85	0.86
PCL+BG10%	171.94±27.83	171.14±27.83	170.96±74.81	1.78
PCL+BG15%	182.74±35.30	182.21±20.07	181.30±1.44	1.34
PCL+HA2%	127.80±7.38	127.60±8.48	126.82±10.54	1.18
PCL+HA5%	179.30±23.43	178.49±22.33	178.22±10.02	1.34
PCL+HA10%	207.33±26.48	207.33±31.27	206.72±33.35	0.98
PCL+HA15%	211.34±50.00	211.12±85.70	210.83±26.05	1.34

(*p<0.05 significant compared Initial with other time periods)

Table shows comparison of Mean Elongation at break within the groups at different time periods ie initial, After 14 days of degradation and After 28 days of degradation in PBS. All the membranes exhibited a mean reduction in Elongation at break after 14 days and 28 days when compared with the initial value. But the reduction showed by PCL membrane was statistically significant with a p value of 0.05 .

Table-15: Comparison of Initial Mean Weight between the groups

Groups	Initial Weight [mm] (MEAN±SD)	Compared with	p value
PCL	0.008±0.02	[PCL+BG5%,10%,15%], [PCL+HA10%,15%]	0.04
PCL+BG2%	0.009±0.02	[PCL+BG5%,10%,15%], [PCL+HA2%,5%,10%,15%]	0.03
PCL+BG5%	0.005±0.01	PCL+HA2%	0.05
PCL+BG10%	0.005±0.01	PCL+HA2%	0.05
PCL+BG15%	0.005±0.01	PCL+HA2%	0.05
PCL+HA2%	0.007±0.01	PCL+HA10%	0.04
PCL+HA5%	0.006±0.01	PCL+HA10%	0.05
PCL+HA10%	0.004±0.01	PCL+HA15%	0.67
PCL+HA15%	0.005±0.02		

(p<0.05 considered statistically significant compared between the groups)

Table shows comparison of mean initial weight between the groups. Among the groups, PCL+BG2% showed higher weight [0.009±0.02gms] and was statistically significant when compared with [PCL+BG5%,10%,15%], [PCL+HA10%,15%]. The mean weight of PCL was 0.008 gms and was statistically significant. Among the PCL+BG group lower weight was exhibited by PCL+BG5%,10%. Among the PCL+HA group PCL+HA2% [0.007±0.01gms] exhibited higher weight.

Table-16: Comparison of Mean Weight loss between the groups after one month

Groups	Final weight[mm] (MEAN±SD)	Compared with	p value
PCL	0.007±0.01	[PCL+BG5%,10%,15%],[PCL+HA10%,15%]	0.04
PCL+BG2%	0.009±0.01	[PCL+BG5%,10%,15%],[PCL+HA2%, 5%,10%,15%]	0.04
PCL+BG5%	0.005±0.01	PCL+HA2%	0.05
PCL+BG10%	0.005±0.02	PCL+HA2%	0.05
PCL+BG15%	0.005±0.01	PCL+HA2%	0.05
PCL+HA2%	0.007±0.01	PCL+HA10%,15%	0.04
PCL+HA5%	0.006±0.02	PCL+HA10%	0.05
PCL+HA10%	0.004±0.01	PCL+HA15%	1.89
PCL+HA15%	0.005±0.01		

(p<0.05 considered statistically significant compared between the groups)

The table shows comparison of mean weight loss between the groups after one month of degradation in PBS. Among the groups,PCL+BG2% showed higher weight [0.009±0.01gms] and was statistically significant when compared with [PCL+BG5%,10%,15%], [PCL+HA2%,5%,10%,15%]. The mean weight of PCL was 0.007 gms and was statistically significant. Among the PCL+BG group lower weight was exhibited by PCL+BG5%,15%. Among the PCL+HA group PCL+HA2% [0.007±0.01gms] exhibited higher weight.

Table-17: Comparison of Mean weight loss within the groups at different time periods

Groups	Initial Weight[mm] (MEAN±SD)	Weight after one month [mm] (MEAN±SD)	p value
PCL	0.008±0.02	0.007±0.01	0.56
PCL+BG2%	0.009±0.02	0.009±0.01	1.78
PCL+BG5%	0.005±0.01	0.005±0.01	1.45
PCL+BG10%	0.005±0.01	0.005±0.02	1.45
PCL+BG15%	0.005±0.01	0.005±0.01	1.45
PCL+HA2%	0.007±0.01	0.007±0.01	1.67
PCL+HA5%	0.006±0.01	0.006±0.02	1.36
PCL+HA10%	0.004±0.01	0.004±0.01	1.78
PCL+HA15%	0.005±0.02	0.005±0.01	1.45

(p<0.05 considered statistically significant compared between the groups)

Table shows comparison of Mean weight loss within the groups at different time periods. On comparing, none of the membrane exhibited significant weight loss. Initial weight of the membrane remains constant after one month for all the membranes except for PCL [0.008±0.02gms reduced to 0.007±0.01gms].

Table-18: Comparison of Initial Mean Thickness between the groups

Groups	Initial thickness[mm] (MEAN±SD)	Compared with	p value
PCL	0.04±0.01	PCL+BG10%,15%	0.05
PCL+BG2%	0.05±0.02	PCL+BG10%,15%	0.05
PCL+BG5%	0.06±0.01	[PCL+BG10%,15%], [PCL+HA2%, 5%,10%,15%]	1.34
PCL+BG10%	0.07±0.01	PCL+HA2%	0.05
PCL+BG15%	0.08±0.02	PCL+HA2%	0.05
PCL+HA2%	0.04±0.01	PCL+HA5%,10%,15%	1.23
PCL+HA5%	0.05±0.01	PCL+HA10%,15%	1.34
PCL+HA10%	0.06±0.01	PCL+HA15%	1.56
PCL+HA15%	0.06±0.01		

(p<0.05 considered statistically significant compared between the groups)

Table shows the initial mean thickness of all the membranes. Among the membranes, PCL+BG15% showed higher thickness[0.08±0.02mm] but was significant only when compared with PCL+HA2% [0.04±0.01mm]. Least thickness was shown by PCL and PCL+HA2% [0.04±0.01mm] membrane and was statistically significant only on comparing with PCL+BG10% [0.07±0.01mm]and PCL+BG15%[0.08±0.02mm].

Table-19: Comparison of Mean Thickness between the groups at 14 days

Groups	Initial thickness [mm] (MEAN±SD)	Compared with	p value
PCL	0.04±0.01	PCL+BG10%,15%	0.05
PCL+BG2%	0.04±0.02	PCL+BG10%,15%	0.04
PCL+BG5%	0.06±0.01	[PCL+BG10%,15%], [PCL+HA2%,5%,10%,15%]	1.34
PCL+BG10%	0.07±0.01	PCL+HA2%	0.05
PCL+BG15%	0.08±0.02	PCL+HA2%	0.05
PCL+HA2%	0.04±0.01	PCL+HA5,10%,15%	1.98
PCL+HA5%	0.05±0.01	PCL+HA10%,15%	1.56
PCL+HA10%	0.05±0.01	PCL+HA15%	1.32
PCL+HA15%	0.06±0.01		

(p<0.05 considered statistically significant compared between the groups)

Table shows mean thickness of membranes between the groups after 14 days of degradation. PCL and PCL+BG2% membranes showed mean thickness of 0.04±0.01 and 0.04±0.02 respectively and was statistically significant on comparing with PCL+BG10%,15%. Among the PCL+HA group, PCL+HA15% exhibited higher thickness but was not statistically significant.

Table-20: Comparison of Mean Thickness between the groups after 28 days

Groups	Initial thickness [mm] (MEAN±SD)	Compared with	p value
PCL	0.03±0.01	PCL+BG10%,15%	0.04
PCL+BG2%	0.03±0.02	PCL+BG10%,15%	0.04
PCL+BG5%	0.05±0.01	[PCL+BG10%,15%], PCL+HA2%,5%,10%,15%	1.45
PCL+BG10%	0.07±0.01	PCL+HA2%	0.05
PCL+BG15	0.07±0.01	PCL+HA2%	0.05
PCL+HA2%	0.04±0.01	PCL+HA5%,10%,15%	1.34
PCL+HA5%	0.04±0.01	PCL+HA10%,15%	1.89
PCL+HA10%	0.04±0.01	PCL+HA15%	1.57
PCL+HA15%	0.05±0.04		

(p<0.05 considered statistically significant compared between the groups)

Table shows mean thickness of membranes between the groups after 28 days of degradation. PCL and PCL+BG2% membranes showed mean thickness of 0.03±0.01 and 0.03±0.02 respectively and was statistically significant on comparing with PCL+BG10%,15%. Among the PCL+HA group, PCL+HA15% exhibited higher thickness but was not statistically significant. Among the PCL+BG group, PCL+BG10%, PCL+BG15% showed higher thickness and was statistically significant.

Table-21: Comparison of Mean Thickness within the groups at different time periods

Groups	Initial thickness[mm] (MEAN±SD)	Thickness at 14 days[mm] (MEAN±SD)	Thickness at 28 days [mm] (MEAN±SD)	p value
PCL	0.04±0.01	0.04±0.01	0.03±0.01	1.45
PCL+BG2%	0.05±0.02	0.04±0.02	0.03±0.02	1.23
PCL+BG5%	0.06±0.01	0.06±0.01	0.05±0.01	0.56
PCL+BG10%	0.07±0.01	0.07±0.01	0.07±0.01	0.92
PCL+BG15%	0.08±0.02	0.08±0.02	0.07±0.01	1.34
PCL+HA2%	0.04±0.01	0.04±0.01	0.04±0.01	1.23
PCL+HA5%	0.05±0.01	0.05±0.01	0.04±0.01	0.89
PCL+HA10%	0.06±0.01	0.05±0.01	0.04±0.01	1.56
PCL+HA15%	0.06±0.01	0.06±0.01	0.05±0.04	1.67

(p<0.05 considered statistically significant compared between the groups)

Table shows mean thickness within the groups at different time periods. Majority of the membranes showed reduced thickness after 28 days when compared with the initial thickness and was not statistically significant[p value >0.05]

Table-22: Comparison of Percentage viability of cells between the groups at 24 hours

Groups	Percentage of viability (%)	Compared with	p value
Cell Control	100	PCL, [PCL+HA2%,15%], [PCL+BG2%,15%]	0.03
PCL	88.45	PCL+HA2%, [PCL+BG2%,15%]	0.04
PCL+HA2%	95.38	PCL+HA15%, PCL+BG15%	0.04
PCL+HA15%	88.99	PCL+BG2%	0.03
PCL+BG2%	97.74	PCL+BG15%	0.04
PCL+BG15%	89.97		

(p<0.05 considered statistically significant compared between the groups)

PCL Membrane exhibited 88.45% cell viability and was statistically significant when compared to control and also with PCL+HA2%, PCL+BG2%, PCL+BG15%. Among the composite membranes, PCL+BG2% [97.74%] showed higher percentage of viability after 24 hours and PCL+HA15% [88.99%] showed least percentage of viable cells and was statistically significant. So on comparison composite membranes exhibited enhanced cell viability than PCL membrane alone.

DIRECT CONTACT-24 HRS WITH L-929 MOUSE FIBROBLASTS

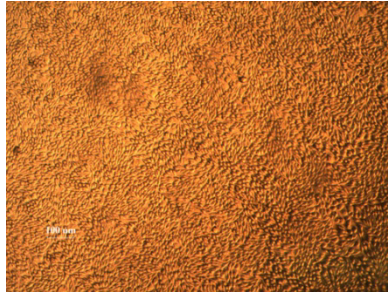


**Image 28.
CONTROL**

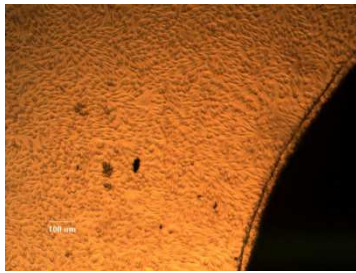


**Image 29.
PCL**

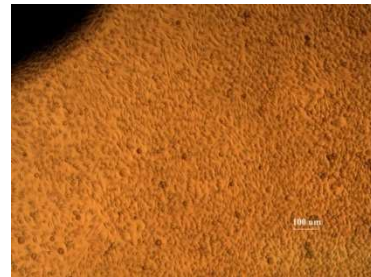


**Image 30.
PCL+HA2%**



**Image 31.
PCL+HA15%**



**Image 32.
PCL+BG2%**



**Image 33.
PCL+BG15%**

MTT ASSAY -24 HRS WITH L-929 MOUSE FIBROBLASTS



**Image 34.
CONTROL**

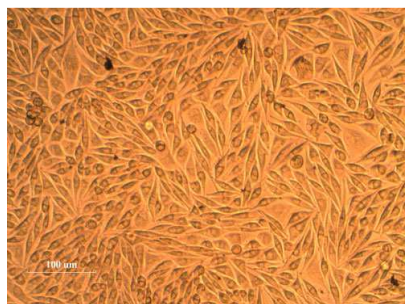


**Image 35.
PCL**

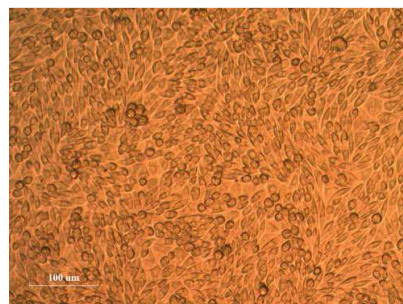


**Image 36.
PCL+HA2%**

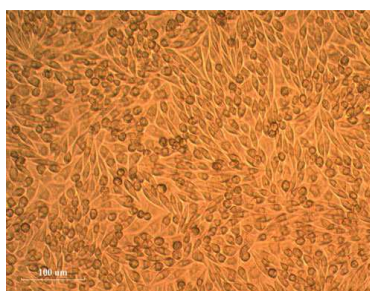
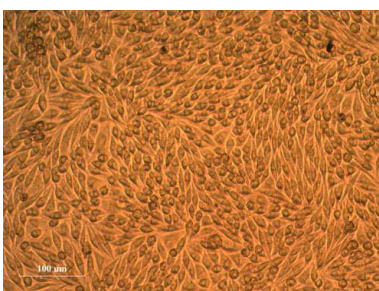
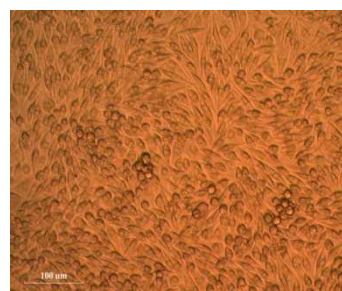


Image 37. PCL+HA15%



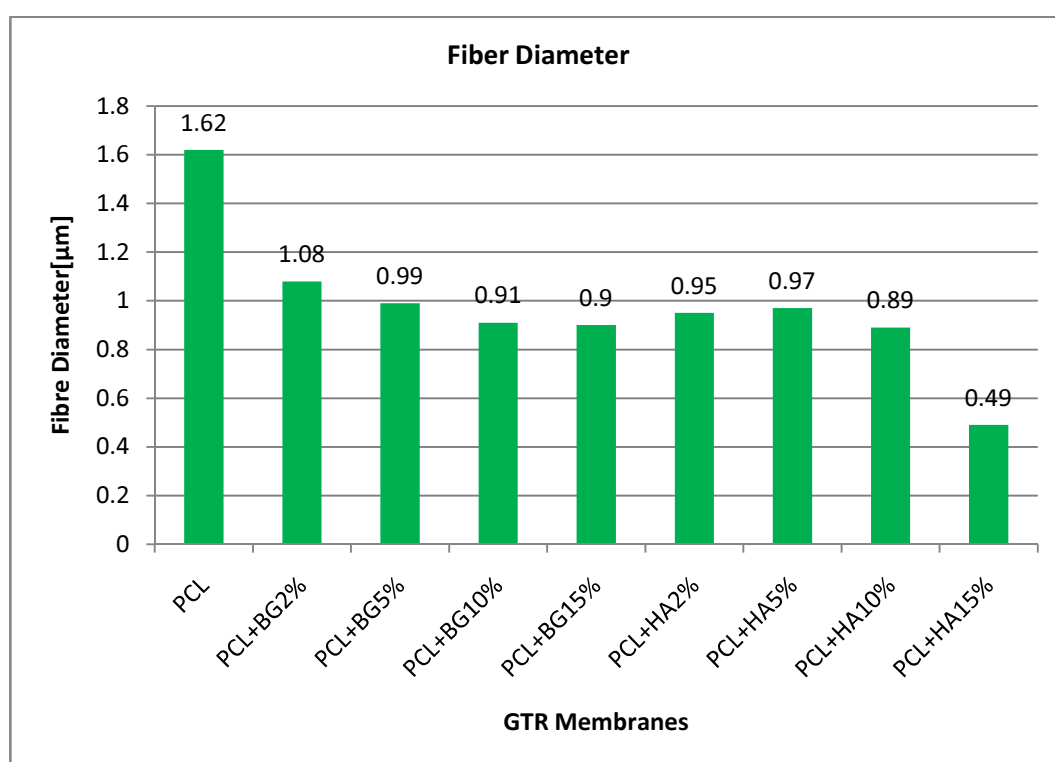
**Image 38.
PCL+BG2%**



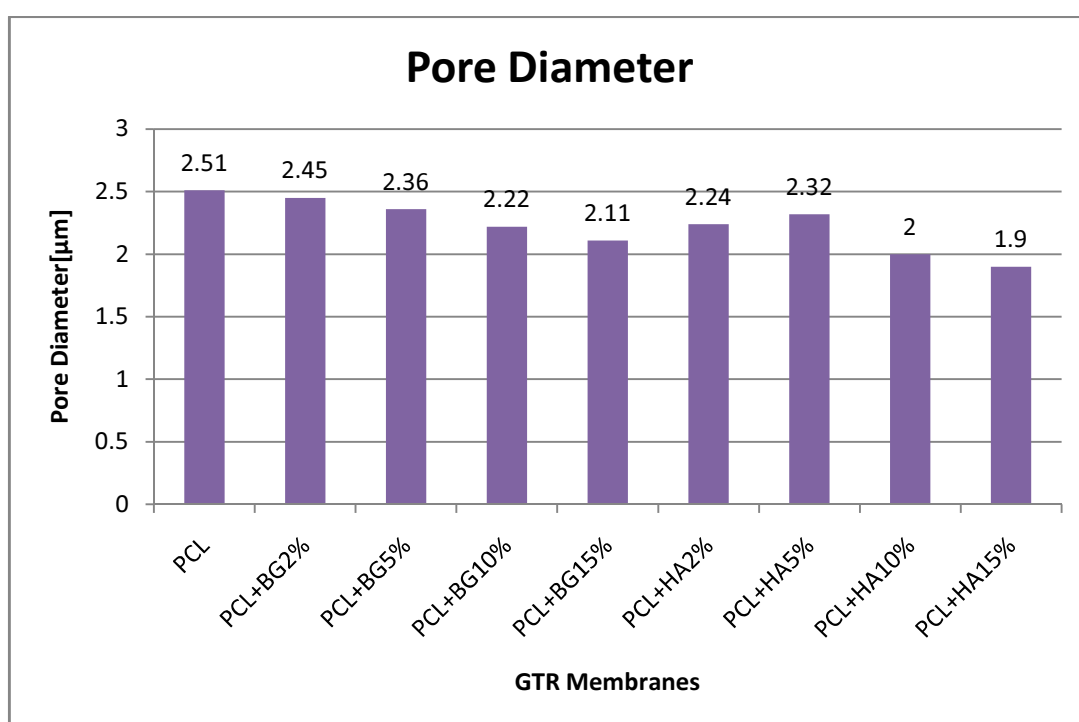
**Image 39.
PCL+BG15%**

GRAPHS

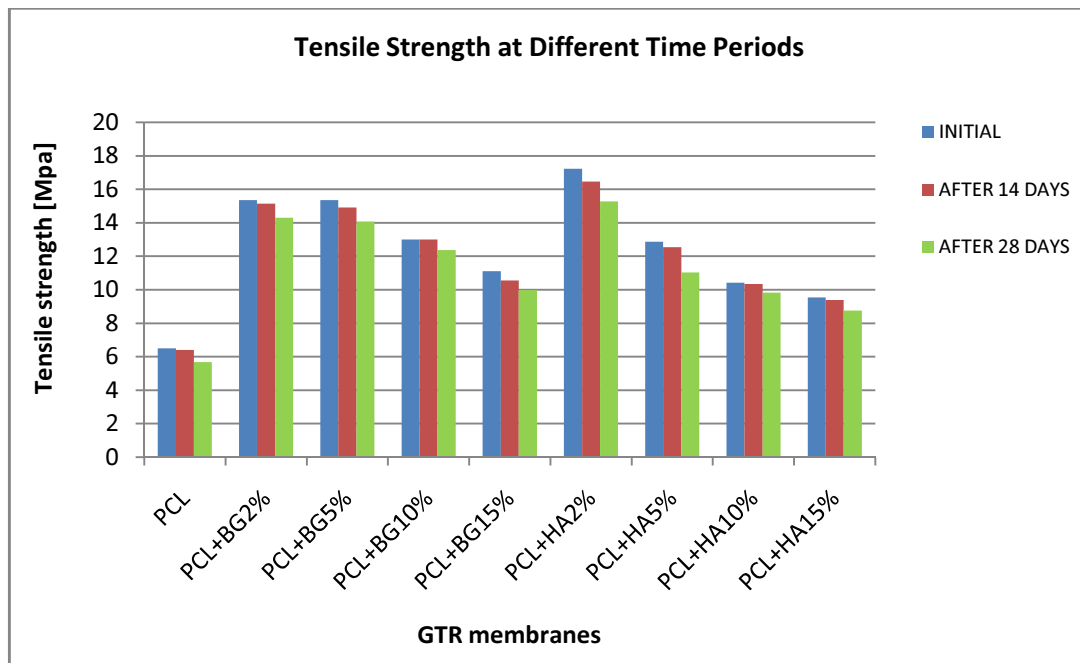
Graph-1. Comparison of Mean Fiber diameter between the groups



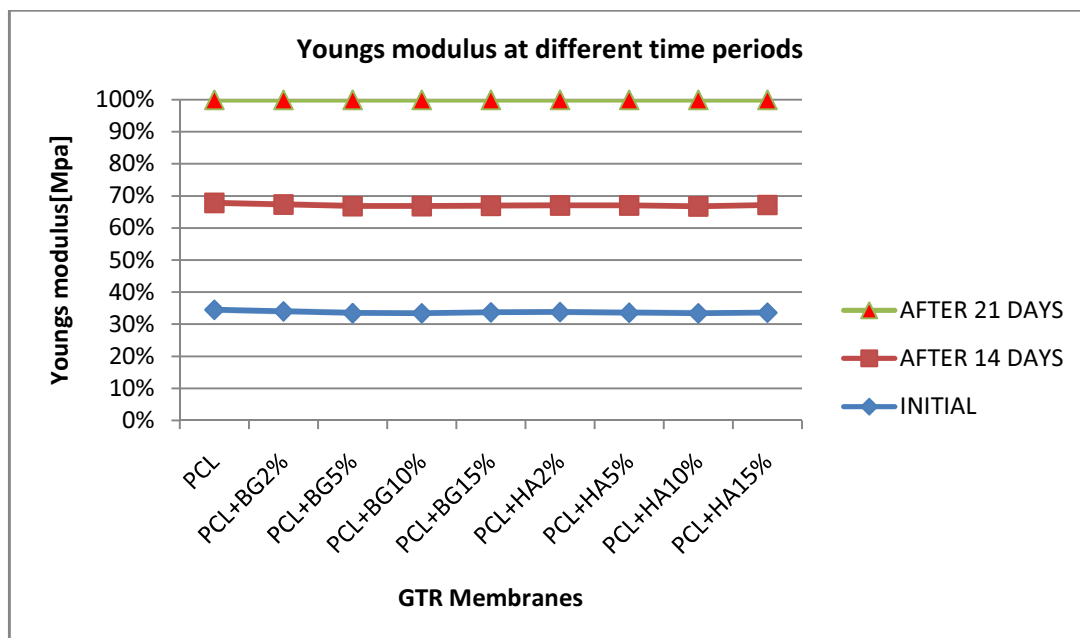
Graph-2. Comparison of Mean Pore diameter between the groups



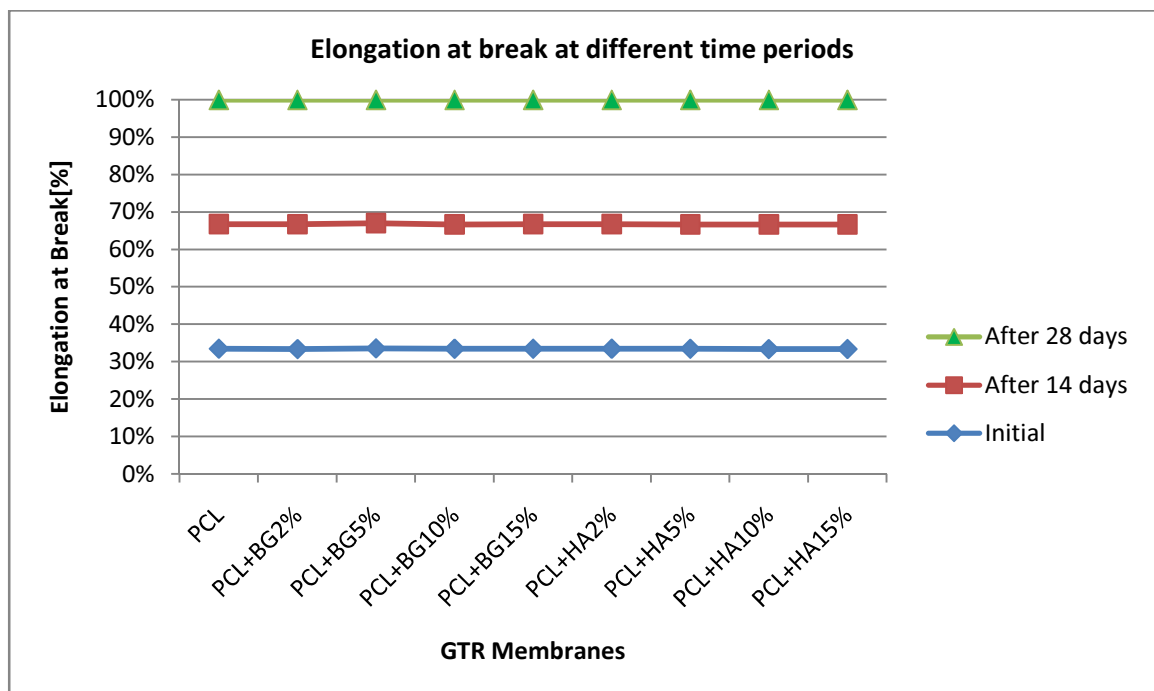
Graph-3. Comparison of Mean Tensile strength within the groups at different time periods



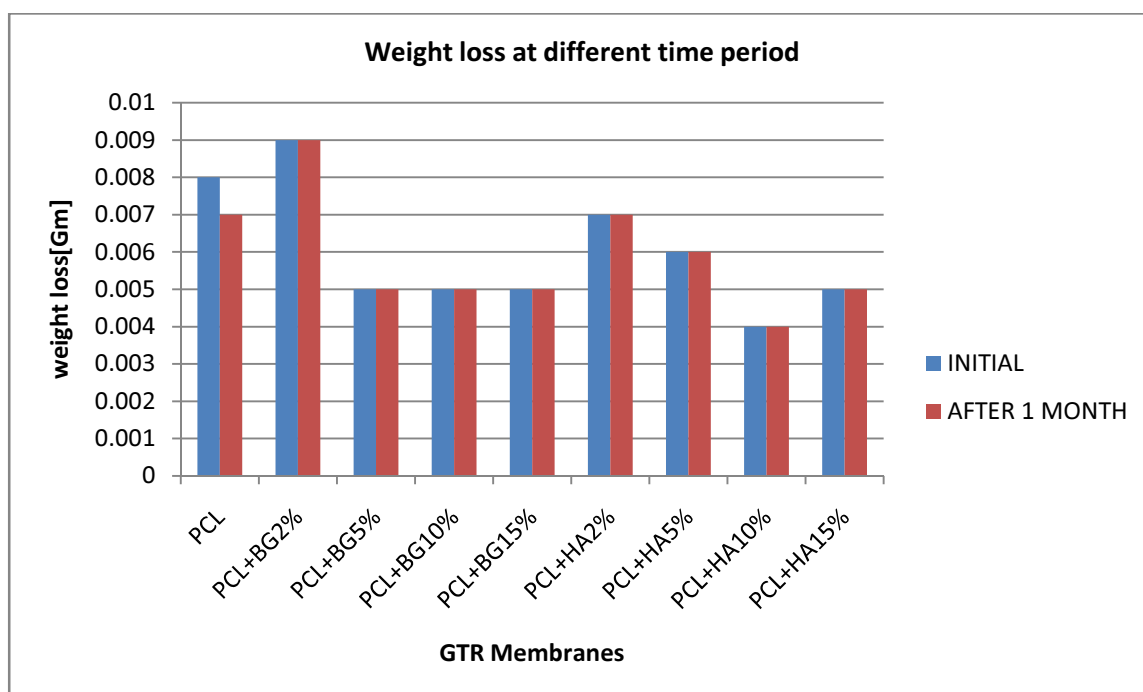
Graph-4. Comparison of Mean Youngs modulus within the groups at different time periods



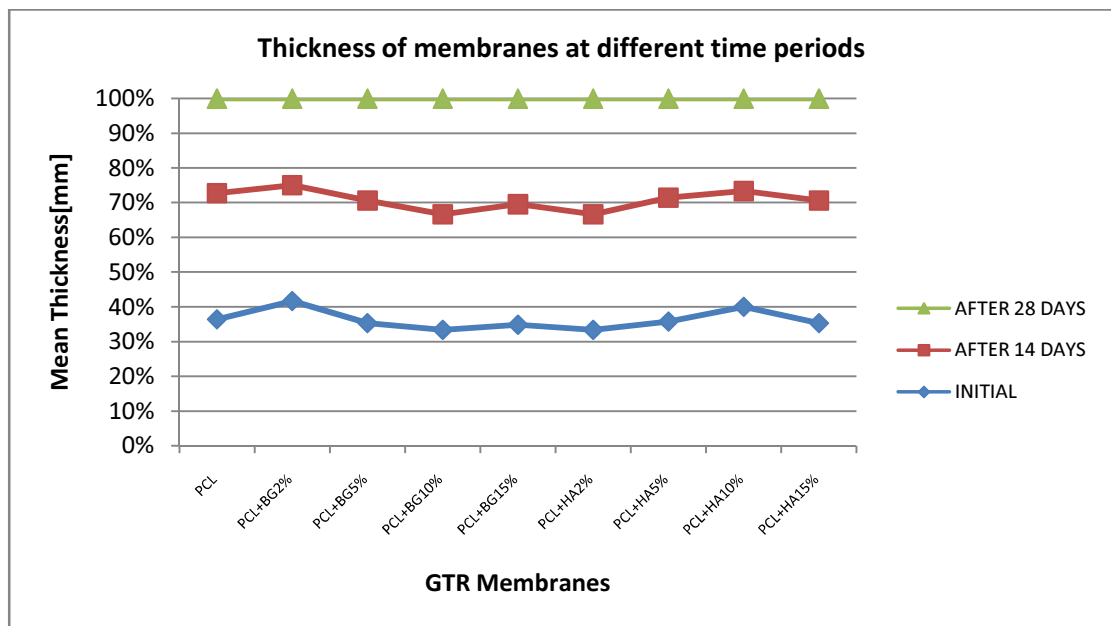
Graph-5. Comparison of Mean Elongation at break within the groups at different time periods



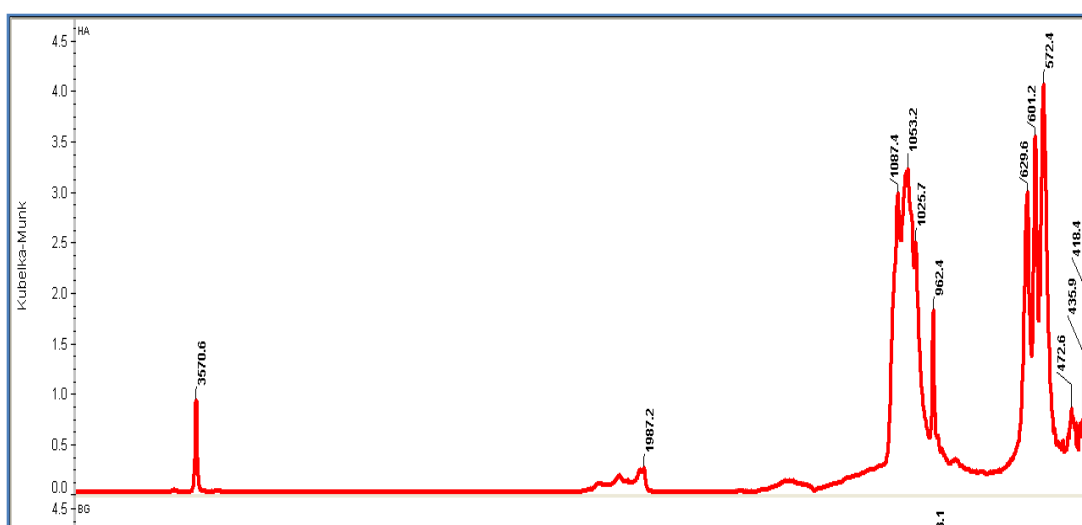
Graph-6. Comparison of Mean weight loss within the groups at different time periods



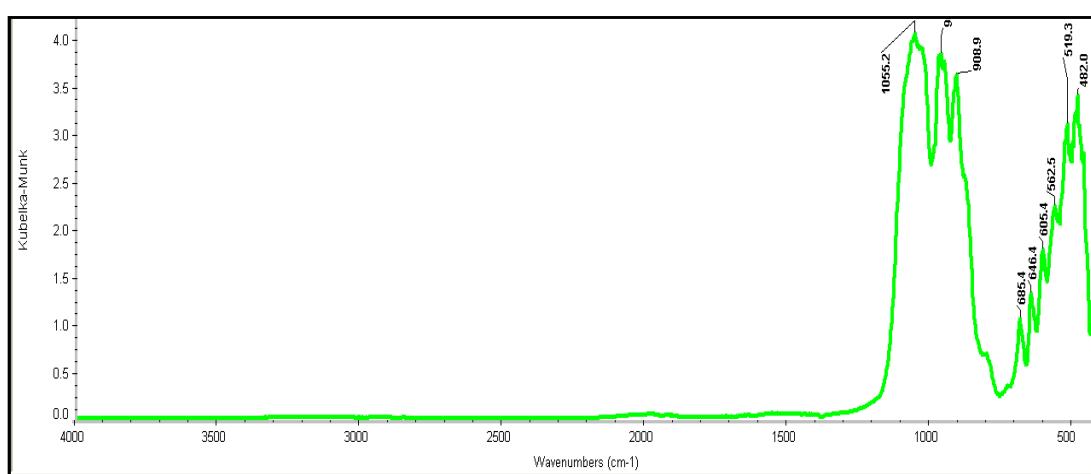
Graph-7. Comparison of Mean Thickness within the groups at different time periods



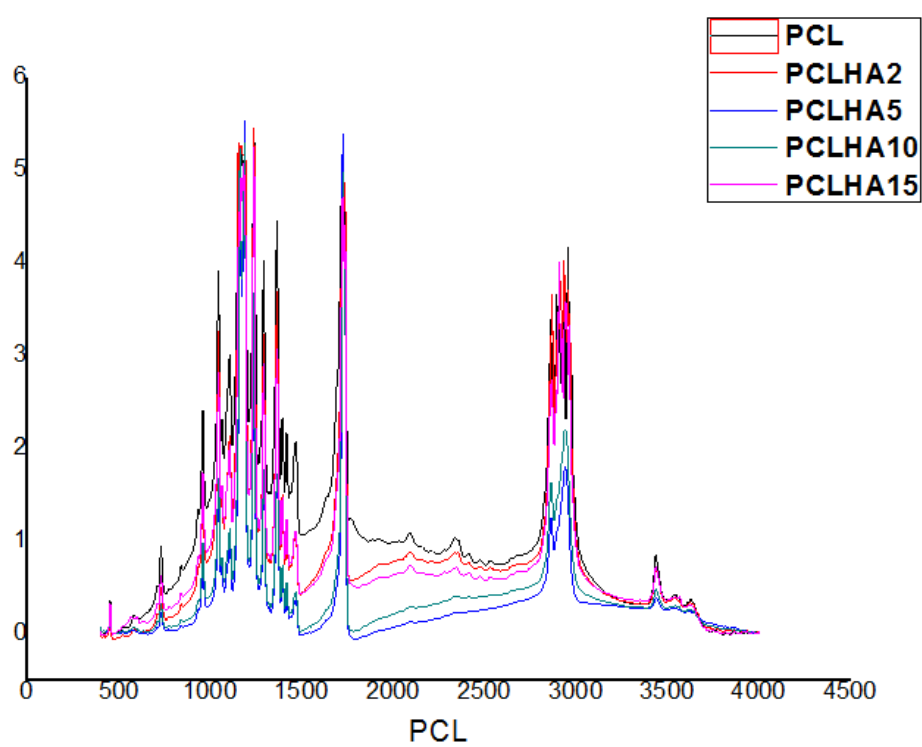
Graph-8. FTIR analysis of Hydroxyapatite



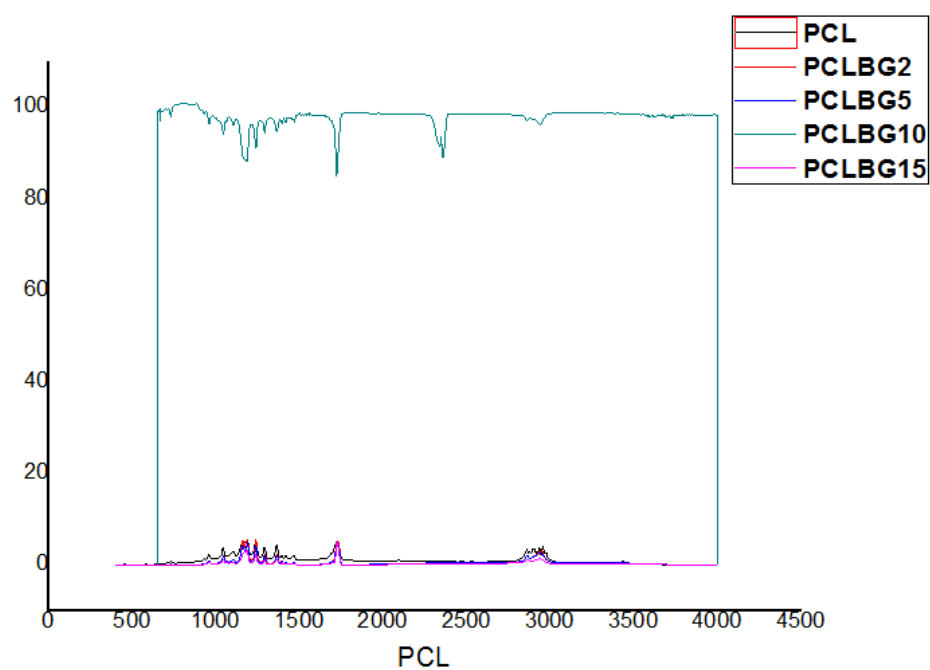
Graph-9. FTIR analysis of BG



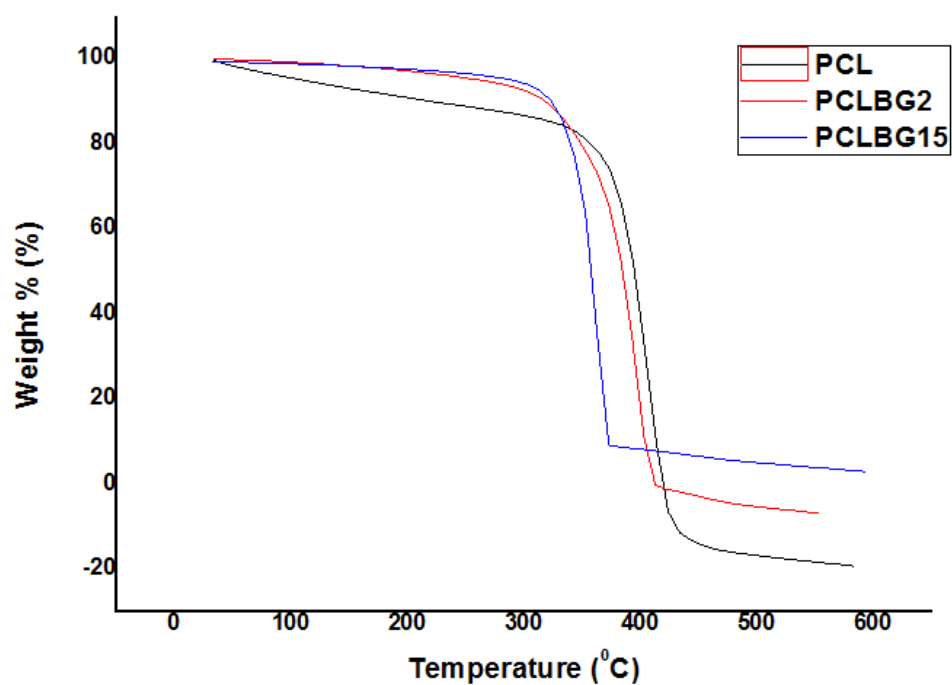
Graph-10. FTIR analysis of PCL + HA



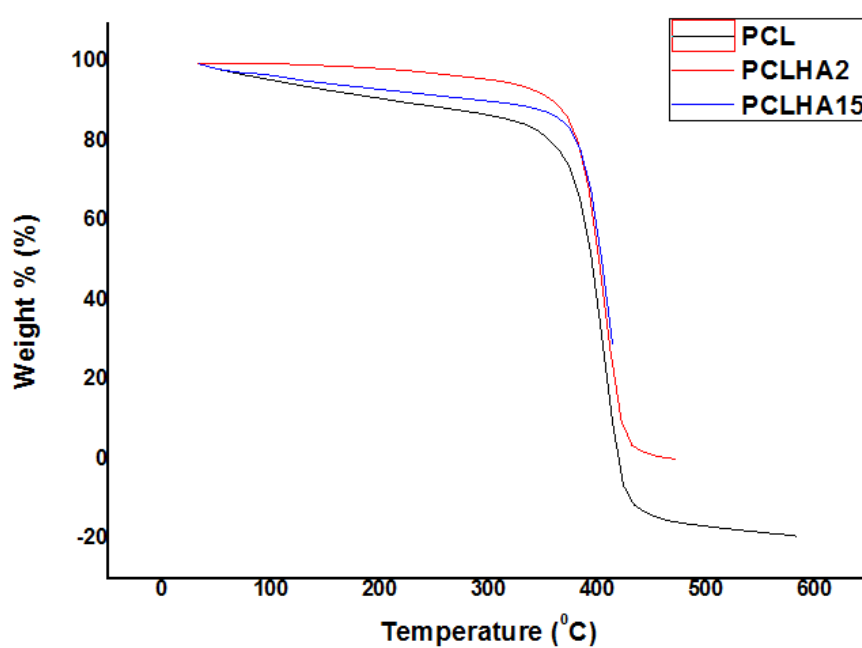
Graph-11. FTIR ANALYSIS of PCL + BG



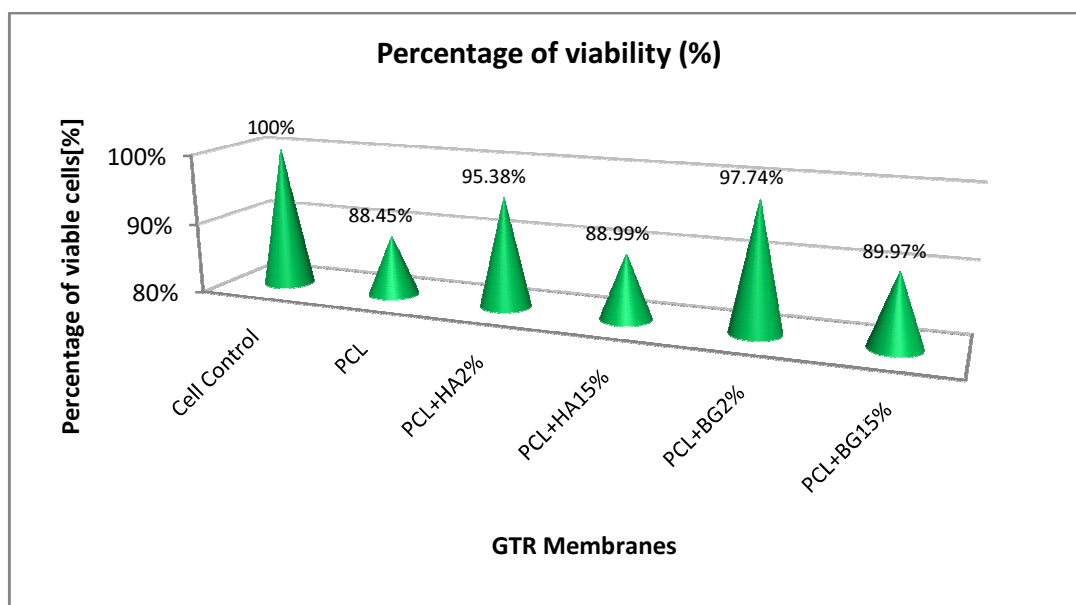
Graph-12. TGA of PCL + BG



Graph-13. TGA of PCL + HA



Graph-14. Comparison of Percentage viability of cells between the groups at 24 hours



DISCUSSION

Periodontal disease is a chronic inflammatory condition which, if untreated, may ultimately result in tooth loss due to the destruction of the surrounding soft and hard tissues.^{46,47} Periodontal regeneration following surgical treatment requires the reconstitution of the complex structure of the periodontium, which includes formation of periodontal ligament fibres and their insertion into newly formed cementum on the root surface, as well as regeneration of the adjacent alveolar bone. Guided Tissue Regeneration (GTR) (Gottlow et al. 1986, 1990) has emerged as the most widely used regenerative procedure, and relies on the fulfilment of three main principles: wound stabilization, space maintenance and selective cell repopulation of the defect. This technique consists of the placement of an occlusive barrier membrane over the periodontal defect. By this means, cells capable of regenerating the periodontium, namely periodontal ligament cells as well as osteoblasts and their progenitors, are permitted to infiltrate the defect, whereas cell types unable to support regeneration, such as gingival and epithelial cells, are excluded from the regenerating periodontal defect. By selectively allowing competent cells into the defect, GTR-based therapy results in a more effective healing when compared with non-selective procedures, where a poorly or nonorganized collagenous scar tissue is observed, characterized by epithelial down-growth along the root surface which prevents the formation of periodontal attachment.^{48,49}

In order for a barrier material to function optimally, it has to meet certain essential design criteria^{50,51}

1. Bio-compatibility-The material should not elicit an immune response, sensitization or chronic inflammation which may interfere with healing and present a hazard to the patient.

2. Cell-occlusiveness-The material should act as a barrier to exclude undesirable cell types from entering the secluded space adjacent to the root surface.
3. Tissue integration- The goal of tissue integration is to prevent rapid epithelial downgrowth on the outer surface of the material or encapsulation of the material, and to provide stability to the overlying flap.
4. Space-making- Barrier material is capable of creating and maintaining a space adjacent to the root surface. This will allow the ingrowth of tissue from the periodontal ligament.
5. Clinical manageability- It should be provided in configurations which are easy to trim and to place.

The barrier membranes used for GTR can be broadly divided into three generations of membranes. The first generation of barrier membranes were non resorbable membranes such as titanium reinforced ePTFE, high-density-PTFE, or titanium mesh which are aimed to achieve a suitable combination of physical properties to match those of the replaced tissue with a minimal toxic response in the host. The major drawback is the need for second surgery for the removal of the membrane. The second generation of barrier membranes was designed to be resorbable to avoid the need for surgical removal. There are two broad categories of bioresorbable membranes: the natural and the synthetic membranes. Natural membranes are made of collagen or chitosan. Synthetic barrier materials made of polyesters (e.g, poly(glycolic acid) (PGA), poly(lactic acid) (PLA), poly(-caprolactone) (PCL), and their copolymers) were used.

Third generation barrier membranes are developed based on the concept of Tissue Engineering. The triad for conventional cell-based tissue engineering involves cells, signalling molecules, and scaffold/supporting matrices.⁵² In this triad, the role of the scaffold is the “niche” of cells, and facilitates the attachment, migration, proliferation, and three-dimensional (3D) spatial organization of the cell population that defines the shape of the tissue that needs regeneration.^{53,54} Briefly they may be considered into the following sub divisions: Barrier membranes with Antimicrobial activity, Barrier membranes with Bioactive materials and Barrier membranes with Growth Factor release⁵². Depending on their origins, they can be sorted into natural polymers, such as xenogeneic-derived collagen, and synthetic polymer materials, for example, poly (lactic acid), and polymer composites, which refer to a combination of two or more different materials to obtain specific mechanical, chemical, and physical properties.

Most of current resorbable synthetic polymer membranes on the market are based on aliphatic polyesters, such as poly(lactic acid) (PLA), poly (glycolic acid) (PGA), poly (ϵ -caprolactone) (PCL), poly (hydroxyl valeric acid), and poly (hydroxyl butyric acid), as well as their copolymers. Due to its biocompatibility, low cost and high mechanical strength, polycaprolactone (PCL) is an attractive biomedical polymer and has been extensively studied in bone tissue engineering. PCL does not produce a local acidic environment during the degradation procedure compared with PLA and PLGA.^{55, 56}

One of the limitations of membranes fabricated with PCL is their poor cell-scaffold interactions due to the inherent hydrophobic nature. This may lead to poor cell adhesion, migration, proliferation, and differentiation during cell culture. Hence

strategies to improve the hydrophilicity of PCL based scaffolds are essential. To overcome these problems, recent research efforts have included the incorporation of bone-like ceramics into the membranes, e.g. hydroxyapatite, tricalcium phosphate and calcium carbonate. In these efforts, nano-sized ceramic particles are of particular interest as they mimic the mineral crystals as present in the natural tissue and have been shown to induce a significant increase in protein absorption and cell adhesion, compared to their micro-sized counterparts.⁵⁷ Although numerous membrane materials have been investigated, few studies have focused on the technique of membrane preparation. So far, most GTR/GBR membranes are made in the shape of porous foam, created by traditional methods such as particulate leaching, solvent casting or gas foaming.^{58, 21}

Recently, a new technique has been introduced, called electrospinning, which allows the preparation of thin fibrous membranes.⁵⁸ Electrospinning, a spinning technique, is a unique approach using electrostatic forces to produce fine fibers from polymer solutions or melts and the fibers thus produced have a thinner diameter (from nanometer to micrometer) and a larger surface area than those obtained from conventional spinning processes. Furthermore, a DC voltage in the range of several tens of Kvs is necessary to generate the electrospinning. This process, mainly based on the principle that strong mutual electrical repulsive forces overcome weaker forces of surface tension in the charged polymer liquid (Chew et al., 2006). Currently, there are two standard electrospinning setups, vertical and horizontal. With the expansion of this technology, several research groups have developed more sophisticated systems that can fabricate more complex nanofibrous structures in a more controlled and

efficient manner (Kidoaki et al., 2005; Stankus et al., 2006).^{58,59,60} Electrospinning is conducted at room temperature with atmosphere conditions. Basically, an electrospinning system consists of three major components: a high voltage power supply, a spinneret (e.g., a pipette tip) and a grounded collecting plate (usually a metal screen, plate, or rotating mandrel) and utilizes a high voltage source to inject charge of a certain polarity into a polymer solution or melt, which is then accelerated towards a collector of opposite polarity (Liang et al., 2007; Sill and Recum, 2008). Most of the polymers are dissolved in some solvents before electrospinning, and when it completely dissolves, forms polymer solution. The polymer fluid is then introduced into the capillary tube for electrospinning.^{61,62,63} In the electrospinning process, a polymer solution held by its surface tension at the end of a capillary tube is subjected to an electric field and an electric charge is induced on the liquid surface due to this electric field. When the electric field applied reaches a critical value, the repulsive electrical forces overcome the surface tension forces. Eventually, a charged jet of the solution is ejected from the tip of the Taylor cone and an unstable and a rapid whipping of the jet occurs in the space between the capillary tip and collector which leads to evaporation of the solvent, leaving a polymer behind. (Taylor, 1969, Yarin et al., 2001; Adomaviciute and Milasius, 2007). The jet is only stable at the tip of the spinneret and after that instability starts.^{58,64-67} Thus, the electrospinning process offers a simplified technique for fiber formation. Fibers obtained from electrospinning are in the range of 50 nm to a few microns in diameter and generally collected in the form of a non-woven structure. It has already been shown that electrospun membranes have the potential to promote osteoblastic cell function and bone regeneration.⁵⁷

In the present study, 3 different GTR membranes are made grouped as PCL, PCL+BG and PCL+HA. PCL+BG and PCL+HA consisted of membranes fabricated with 4 different weight concentrations of BG/HAP ie PCL+BG2%, PCL+BG5%, PCL+BG10% and PCL+BG15%. Similarly PCL+HA group also consisted of PCL+HA2%, PCL+HA5%, PCL+HA10% and PCL+HA15%. Morphological evaluation of the fabricated membranes was done using SEM. There was statistically significant difference in Fiber and Pore diameter for PCL membrane and also for PCL+HA2%, PCL+HA5%, PCL+HA10%, PCL+HA15% and PCL+BG2%, PCL+BG5%, PCL+BG10%, PCL+BG15% GTR membranes [Table 1,2: Image 1-27]. For PCL, non uniform fibers with an average diameter of $1.62\text{ }\mu\text{m}$ and pore diameter of $2.51\text{ }\mu\text{m}$ were obtained. As evident from the SEM micrograph blending PCL with different weight concentrations of BG and nHAP resulted in reduction of fiber diameters and pore diameter. Among the PCL blended with BG and nHAP membranes, PCL+BG2% showed statistically significant increased fiber diameter [$1.08 \pm 0.16\text{ }\mu\text{m}$] and pore diameter [$2.45 \pm 0.92\text{ }\mu\text{m}$]. The fiber diameter and pore diameter was very less for PCL+HA15% [$0.49 \pm 0.58\text{ }\mu\text{m}$ and $1.90 \pm 0.67\text{ }\mu\text{m}$ respectively]. Overall the fibers showed decreased fiber and pore diameter with addition of different weight concentrations of filler particles when compared to PCL fibers alone [Graph-1,2]. These findings of the present study was consistent with the study done by Remya et al in 2013 where the fabricated PCL membrane had a fiber diameter of $1.54\text{ }\mu\text{m}$.

Electrospinning technique is governed by various processing parameters such as solution viscosity, applied potential, flow rate, tip to collector distance, solvent nature, needle diameter and various ambient parameters. In the present

study, spinning was done at a predetermined optimized condition to get bead free fibers. It is observed that blending PCL with different concentrations of bioactive materials resulted in smooth fibers with reduced fiber diameter. This reduction in fiber diameter can be attributed to difference in solution viscosity i.e when viscosity decreases conductivity increases and this conductivity is inversely proportional to fiber diameter. A reduction in fiber diameter was observed with the incorporation of nHAP particles and this can be attributed to the presence of calcium and phosphate ions in nHAP which provides higher conductivity.²¹

Pore diameter and fiber diameter plays a vital role in the biological performance of scaffold as it determines both cell–cell as well as cell– membrane interaction. High porosity, adequate pore size and interconnected pore network are essential criteria for a tissue engineering as it enables better cell infiltration and vascularization.^{21,68} The reduction in pore size occurs as more layers of fibers might overlap with each other, especially when the fiber diameter is smaller, resulting in smaller pore diameter. The pore size distribution lies in a range below 300µm for all the scaffolds. The preferable pore size for osteoblast cells ranges from 200 to 400 µm for encouraging migration, attachment and proliferation. However for electrospun matrices pores formed are much smaller than the normal cell size of a few to tens of micrometer. Pores in an electrospun structure are formed by the randomly oriented fibers lying loosely upon each other. Cells can migrate through pores by their amoeboid movement and can push surrounding fibers aside to expand the hole. This dynamic architecture of fibers allows cells to adjust according to pore size and grow into nanofiber matrices.²¹

In this study PCL+BG2% showed statistically significant increased fiber diameter [$1.08 \pm 0.16\mu\text{m}$; $p<0.03$] and pore diameter [$2.45\pm0.92\mu\text{m}$; $p<0.04$] when compared to other membranes.

The mechanical properties of the fabricated GTR membranes observed in this study included Tensile strength, Youngs Modulus, and Elongation at break. All the membranes exhibited statistically significant difference in Mechanical properties between and within the groups. Among the different GTR membranes, higher tensile strength was exhibited by PCL+HA2% [$17.22\pm2.80\text{ MPa}$] and PCL+HA15% showed the least tensile strength [9.55 ± 1.04]. These superiority in their tensile strength were maintained by the membranes initially, after 14 days and one month after degradation in PBS. and was statistically significant[Table 3,4,5,6][Graph-3]. These values that we obtained in our study are higher than the values of Tensile strength obtained by Yang et al.⁵⁸ and Yunzhu et al.⁷⁰ In case of Youngs modulus[Table 7,8,9,10], PCL+HA2% exhibited the highest Youngs modulus [57.16 ± 7.39] and the least was exhibited by PCL [$28.01\pm5.98\text{MPa}$] initially, after 14 days and one month after degradation in PBS[Graph-4] which was consistent with the studies done by Yang et al where Youngs modulus was about 19.46MPa for PCL+HA composite membranes. In surgery, GTR membranes are tightly fixed by biodegradable pins, medical glue or sutures preventing them from sagging into bone defects. Our mechanical test showed that the addition of nHAP increased the mechanical properties of the PCL membrane. Among the different membranes that we tested in this study, the PCL+HA2% and PCL+BG2% showed the highest tensile strength, and Youngs modulus. With an increasing nHAP content, the higher concentrations of PCL+BG and PCL+HA [5%,10%,15%] showed weakened

properties compared with PCL+HA2% but remained stronger and tougher than the pure PCL membrane. This mechanical reinforcement effect can be attributed to an additional energy-dissipating mechanism introduced by the nanoparticles in PCL. Recent molecular dynamics studies suggested that this additional dissipative mechanism is a result of the mobility of the nanoparticles. During the deformation process the nanoparticles orient and align under tensile stress, creating temporary cross-links between polymer chains, thereby creating a local region of enhanced strength. However, when the size of the nHAP/BG stacks is increased, they become less mobile. Therefore, the ability of the nHAP/BG to dissipate energy is also reduced, resulting in almost no improvement in the toughness of the material.⁵⁸ Findings from our study was consistent with the study done by Remya et al in 2013 which states that membranes with smaller fiber diameters will provide higher overall relative bonded areas between fibers due to the increased surface area, bonding density, and better distribution of bonds.²¹

Considering elongation at break or elasticity of the fabricated GTR membranes, highest elongation at break was exhibited by PCL [259.25±6.95 %] and least was exhibited by PCL+HA2% [127.80±7.38] initially, after 14 days and one month after degradation in PBS [Table 11,12,13,14] and was statistically significant[Graph-5]. Elasticity of a material is inversely proportional to the strength, i.e PCL+HA2% had increased tensile strength so the membrane exhibited least Elasticity/elongation at break. All the membranes maintained its initial superiority in mechanical properties even after one month of invitro degradation in PBS.

To the best of our knowledge no studies have evaluated the thickness and weight of the Electrospun GTR membrane before and after invitro degradation.

Among the different GTR membranes, mean higher weight was showed by PCL+BG2% [$0.009\pm0.01\text{gm}$] and lower weight by PCL+HA10% [$0.004\pm0.01\text{gm}$] [Table 15,16,17] and the differences between them was statistically significant [Graph-6]. We speculate that this discrepancy can be due to a difference in dispersion of particles. In case of thickness, Highest thickness was showed by PCL+BG15% [$0.08\pm0.02\text{ mm}$] and least thickness was showed by PCL [$0.04\pm0.01\text{mm}$] [Table 18,19,20,21] which was statistically significant [Graph-7] which is attributed to increased weight concentrations of Bioactive materials.

Evaluating the chemical stability of the fabricated membranes by FTIR ,the spectra revealed that PCL exhibited its characteristic absorption bands for C=O stretching vibrations from ester bond at 1732 cm^{-1} , CH₂ stretching vibrations at 2973 cm^{-1} and 2861 cm^{-1} and that of C-O vibrations from ether groups at 1240 cm^{-1} respectively. Similarly the FTIR spectrum of HA showed characteristic functional groups of phosphate and hydroxyl moieties. Phosphate peaks were observed between 570 cm^{-1} and 1050 cm^{-1} (572.4 cm^{-1} , 601.2 cm^{-1} , 987.2 cm^{-1} , 1053cm^{-1}). The characteristic hydroxyl peak was observed at 3570.6 cm^{-1} . The FTIR spectrum of BG showed characteristic functional groups of silicate absorption bands assigned to the peaks 1055 , 908 and 482 cm^{-1} , respectively: asymmetric stretching mode, symmetric stretching vibration and rocking vibration of Si–O– S[Graph-8,9,10,11]

The inference from FTIR analysis is that HA and BG were successfully incorporated in PCL membrane without any undesirable chemical reaction or loss of chemical structure of all these three components indicated by the appearance of signature peaks of PCL, HA and BG in PCLHA and PCLBG composite membranes. These findings of FTIR analysis were consistent with the study done by Yunzhu et al⁷⁰

The presence of BG and HA in PCL scaffolds was analyzed using thermogravimetric analysis. For PCL, complete charring occurred at 420°C whereas for composite membranes, even after 420°C the weight percentage of filler remaining was of 27% for PCLHA2% and 29% for PCL+HA15% composites and that of 2.2% for PCLBG2% and 7.7% for PCL+BG15% composite membranes [Graph-12,13]. This shows that composites membranes exhibited high thermal stability. The study done by Neethu et al states that complete charring of the PCL occurred at 428°C which was not consistent with our study. The reason for this might be the difference in molecular weight of the PCL they used in that study [Mw70,000 – 90,000].⁷¹

Apart from favorable physicochemical and mechanical properties, the most important requirement for a biomaterial is its biocompatibility in a specific environment, together with the non cytotoxicity of its degradation products.⁷¹ As a preliminary step towards the evaluation of cyto-compatibility of the scaffold, MTT assay was performed and the result reveals the non-cytotoxic nature of the tested membranes i.e PCL, PCL+BG2%, PCL+BG15% and PCL+HA2%, PCL+HA15%. The percentage viability of cells on the membrane determine the suitability of the material for the intended application. In this study the potential of fabricated membranes for tissue engineering applications was evaluated by invitro cell culture studies using L929 Mouse fibroblast cell lines. Quantitative and qualitative assays proved that the fabricated membranes are non toxic. The cells maintained their characteristic spindle morphology on all the GTR Membranes after 24 hours. [Image 27-33] The percentage cell viability was higher in PCL+BG2% [97.74, P<0.04] after 24 hours and was statistically significant when compared with rest of the GTR

membranes[Table-22; Graph-14]. Ogawa et al in 2016⁵⁴ stated that, nano-modification of biomaterials might increase the surface area and adsorption of signaling molecules. In our study, the PCL+BG2% exhibited higher fiber diameter [$1.08\pm0.16\mu\text{m}$]. As a result of this, the membrane showed increased surface area which results in higher percentage of viable cells. [Images34-39]. These observations confirm the bioactivity of the fabricated membranes and its usefulness in periodontal tissue engineering as a GTR membrane for proliferation and differentiation in to specific cell lineage.

Even though the results of present study showed that the Electrospun GTR membranes possessed adequate invitro properties and supported cell attachment, there are certain limitations of the study. The cell part of the study here was of limited size and in the future the membranes should be completely tested using different cell types, e.g. gingival fibroblasts, periodontal ligament fibroblasts and osteoblast-like cells in terms of cell attachment, proliferation, migration, penetration, differentiation and mineralization. Another limitation is, the present study have not used any surfactant in order to achieve a stable and uniform nHAP /BG suspension in the polymer solutions.

SUMMARY

In the present study PCL reinforced with Bioactive Glass/ Nanohydroxyapatite composite membranes were fabricated and their invitro properties were characterized. All the electrospun nanofibrous membranes possessed excellent Mechanical properties initially and after one month of degradation in PBS. Moreover none of the membranes found to be cytotoxic at lower concentrations and higher concentrations. On comparing the overall properties PCL+BG2% exhibited superior cell attachment and percentage of viable cells, increased fiber and pore diameter which satisfies the ideal properties needed for GTR membranes. In case of Tensile strength, PCL+HA2% exhibited a higher mechanical strength than PCL+BG2% but less fiber diameter. Thermal stability and chemical stability analysis showed that the fabricated membranes were stable at higher temperature with presence of bioactive filler particle.

CONCLUSION

The optimal resorbable membrane for GTR or GBR has to be strong, able to stimulate bone formation and promote osteoblast-like cell proliferation and differentiation. In the present study, composite nanofibrous membranes based on nHAP/BG and PCL were prepared by electrospinning. Physiochemical, mechanical and in vitro characterization showed that the composite membrane fulfilled all aforementioned requirements. However, the membrane with a high nHAP/BG loading density was weaker than the one with low nHAP/BG loading density. Based on our results, we conclude that the composite nanofibrous membrane prepared by Electrospinning is suitable for the use as a GTR membrane and it is a useful prototype for further development of a final membrane for clinical use.

BIBLIOGRAPHY

1. Vargas S, Ilyina A, Segura C, Silva B, Mendez G. Etiology and microbiology of periodontal diseases: A review. *Afr J Microbiol Res* 2015;9(48):2300-2306.
2. Laurell L, Gottlow J. Guided tissue regeneration update. *Inter Dent J* 1998;48(4):386-398.
3. Position Paper: Periodontal Regeneration. *J Periodontol* 2005;76(9):1601-1622.
4. Shimauchi H, Nemoto E, Ishihata H, Shimomura M. Possible functional scaffolds for periodontal regeneration. *Jpn Dent Sci Review* 2013;49(4):118-30.
5. Singh AK. GTR membranes: The barriers for periodontal regeneration. *DHR-IJMS* 2013;4(1):31-8.
6. Sam G. Evolution of Barrier Membranes in Periodontal Regeneration-“Are the third Generation Membranes really here?”. *J Clin Diagn Res.* 2014; ZE14–ZE17
7. Cannillo V, Fabbri P, Sola A. Fabrication of 45S5 bioactive glass- polycaprolactone composite scaffolds. *ICCM Int Conf Compos Mater* [Internet]. 2009.
8. Guo B, Lei B, Li P, Ma P. Functionalized scaffolds to enhance tissue regeneration. *Regen Biomater* 2015;2(1):47-57.
9. Prakash Mb, Kumar Nag M, Mohammed A, Bhargavi K, Sai Ram M, Rajkumar R. Poly (ϵ -caprolactone) PCL Scaffolds Preparation and characterization for tissue engineering. *Int J Mech Eng Robot* 2014;1(2):2321–5747.
10. Vasita R, Katti DS. Nanofibers and their applications in tissue engineering. *Int J Nanomedicine* 2006;1(1):15–30.

11. Boccaccini AR, Chatzistavrou X, Yunos DM, Califano V. Biodegradable Polymer-Bioceramic Composite Scaffolds for Bone Tissue Engineering. Proc 17th Int Conf Compos Mater. 2009.
12. Balu R, Singaravelu S, Nagiah N. Bioceramic Nanofibres by Electrospinning. Fibers. 2014;221–39.
13. Aurer A, JorgiE-Srdjak K. Membranes for Periodontal Regeneration. Acta Stomatol Croat 2005;39(1):107-12.
14. Battistella E, Varoni E, Cochis A, Palazzo B, Rimondini L. Degradable polymers may improve dental practice. J Appl Biomater Biomech 2011;9(3):223-31.
15. Azimi B, Nourpanah P, Rabiee M, Arbab S. Poly (lactide -co- glycolide) Fiber: An Overview. J Eng Fiber Fabr [Internet] 2014;9(3):74–90.
16. Naghizadeh F, Sultana N, Abdul Kadir MR, Tengku Md Shihabudin TM, Hussain R, Kamarul T. The fabrication and characterization of PCL/rice husk derived bioactive glass-ceramic composite scaffolds. J Nanomater 2014;2014.p.9.
17. Montero GA, Gluck JM, King MW. Polycaprolactone (Pcl) Nonwoven Mats for Use as Tissue Engineering Scaffolds Generate by Electrospinning Process. Electrospinning process College of Textiles, North Carolina State University, Raleigh.
18. Yang F, Both SK, Yang X, Walboomers XF, Jansen JA. Development of an electrospun nano-apatite/PCL composite membrane for GTR/GBR application. Acta Biomater [Internet]. Acta Materialia Inc.; 2009;5(9):3295–304.

19. Gürbüz S, Demirtaş T, Yüksel E, Karakeçili A, Doğan A, Gümüşderelioğlu M. Multi-layered functional membranes for periodontal regeneration: Preparation and characterization. *Materials Letters*. 2016;178:256-259.
20. Basile MA, D'Ayala GG, Malinconico M, Laurienzo P, Coudane J, Nottelet B, et al. Functionalized PCL/HA nanocomposites as microporous membranes for bone regeneration. *Mater Sci Eng C [Internet]*. Elsevier 2015;48:457-68.
21. Remya KR, Joseph J, Mani S, John A, Varma HK, Ramesh P. Nanohydroxyapatite incorporated electrospun polycaprolactone/polycaprolactone- polyethyleneglycol-polycaprolactone blend scaffold for bone tissue engineering applications. *J Biomed Nanotechnol* 2013;9(9):1483-94.
22. Hassan MI, Mokhtar M, Sultana N, Khan TH. Production of Hydroxyapatite (HA) nanoparticle and HA / PCL Tissue Engineering Scaffolds for Bone Tissue Engineering. *IECBES* 2012; 239-42.
23. Bottino MC, Thomas V, Janowski GM. *Acta Biomaterialia* A novel spatially designed and functionally graded electrospun membrane for periodontal regeneration. *Acta Biomater* 2011;7(1):216-24.
24. Taylor P. Preparation, Characterization and Cell Attachment Studies of Electrospun Multi-Scale Poly (caprolactone) Fibrous Scaffolds for Tissue Engineering. *J Macromol Sci Part A* 2010; 48(1):21-30.
25. Park SA, Hee S, Wan L, Kim D. Fabrication of porous polycaprolactone / hydroxyapatite (PCL / HA) blend scaffolds using a 3D plotting system for bone tissue engineering. *Bioprocess Biosyst Eng* 2011;34(4):505-13

26. Chen J, Lai G, Chang Y. Preparation of Composite Electrospun Nanofibers of Polycaprolactone and Nanohydroxyapatite for Osteogenic Differentiation of Stem Cells. Nanoelectronics Conference (INEC), 2010.
27. Kim J, Lee T, Cho D, Kim B. Solid Free-Form Fabrication-Based PCL/HA Scaffolds Fabricated with a Multi-Head Deposition System for Bone Tissue Engineering. J Biomater Sci 2010;21(6-7):951-62.
28. Porter JR, Henson A, Popat KC. Biomaterials applications. Biomaterials [Internet]. Elsevier Ltd; 2009;30(5):780–8.
29. Zhao J, Guo LY, Yang XB, Weng J. Preparation of bioactive porous HA/PCL composite scaffolds. Appl Surf Sci 2008;255(5 PART 2):2942–6.
30. Venugopal JR, Low S, Choon AT, Kumar AB, Ramakrishna S. Nanobioengineered electrospun composite nanofibers and osteoblasts for bone regeneration. Artif Organs 2008;32(5):388–97.
31. Wutticharoenmongkol P, Pavasant P, Supaphol P. Osteoblastic phenotype expression of MC3T3-E1 cultured on electrospun polycaprolactone fiber mats filled with hydroxyapatite nanoparticles. Biomacromolecules. 2007;8(8):2602–10.
32. Kim S, Hyun Y, Chung D, Heo S, Shin J, Lee J. Biodegradable Porous PCL/HA Scaffolds for Bone Tissue Engineering. Key Engineering Materials 2007;342-343:77-80.
33. Hyun Y, Kim S, Heo S, Shin J. Characterization of PCL/HA Composite Scaffolds for Bone Tissue Engineering. Key Engineering Materials 2007;342-343:109-112.

34. Wutticharoenmongkol P, Sanchavanakit N, Pavasant P, Supaphol P. Preparation and Characterization of Novel Bone Scaffolds Based on Electrospun Polycaprolactone Fibers Filled with Nanoparticles. *Macromolecular Bioscience*. 2006;6(1):70-77.
35. Sanchavanakit N, Wutticharoenmongkol P, Pavasant P, Supaphol P. Preparation and characterization of novel bone scaffolds based on electrospun polycaprolactone fibers filled with nanoparticles. *Macromol Biosci* 2006;6(1):70-7
36. Khil MS, Bhattarai SR, Kim HY, Kim SZ, Lee KH. Novel fabricated matrix via electrospinning for tissue engineering. *J Biomed Mater Res - Part B Appl Biomater* 2005;72(1):117-24.
37. Fereshteh Z, Nooeaid P, Fathi M, Bagri A, Boccaccini AR. Mechanical properties and drug release behavior of PCL/zein coated 45S5 bioactive glass scaffolds for bone tissue engineering application. *Data Br [Internet]. Elsevier*; 2015;4:524–8.
38. Zhang Y, Wei L, Wu C, Miron RJ. Periodontal regeneration using strontium-loaded mesoporous bioactive glass scaffolds in osteoporotic rats. *PLoS One*. 2014;9(8):1–6.
39. Izadi S, Hesarakhi S, Hafezi-Ardakani M. Evaluation Nanostructure Properties of Bioactive Glass Scaffolds for Bone Tissue Engineering. *Adv Mater Res [Internet]*. 2013; 829:289–93.
40. Nanocomposites E, Otadi M, Mohebbi D. The Effect of Bioglass Nanoparticles and Strontium Component on Tensile Strength of Polycaprolactone / Bioglass. 2014;23-4.

41. Poh P, Hutmacher D, Stevens M, Woodruff M. Fabrication and in vitro characterization of bioactive glass composite scaffolds for bone regeneration. *Biofabrication*. 2013;5(4):045005.
42. Radev L, Vladov D, Michailova I, Cholakova E, Fernandes MF V., Salvado IMM. In vitro Bioactivity of Polycaprolactone/Bioglass Composites. *Int J Mater Chem [Internet]*. 2013;3(5):91–8.
43. Jo JH, Lee EJ, Shin DS, Kim HE, Kim HW, Koh YH, et al. In vitro/in vivo biocompatibility and mechanical properties of bioactive glass nanofiber and poly(ϵ -caprolactone) composite materials. *J Biomed Mater Res - Part B Appl Biomater* 2009;91(1):213–20.
44. Bretcanu O, Misra SK, Yunus DM, Boccaccini AR, Roy I, Kowalczyk T, et al. Electrospun nanofibrous biodegradable polyester coatings on Bioglass-based glass-ceramics for tissue engineering. *Mater Chem Phys* 2009;118(2–3):420–6.
45. Lee H, Yu H, Jang J, Kim H. Bioactivity improvement of poly(ϵ -caprolactone) membrane with the addition of nanofibrous bioactive glass. *Acta Biomaterialia*. 2008;4(3):622–629.
46. Newman MG, Takei HH, Klokkevold PR, Carranze FA. Carranza's Clinical Periodontology. 11th Edition. India: Elsevier Saunders; 2012.
47. Vargas SAI, Ilyina A, Segura CEP, Silva BY, et al. Etiology and microbiology of periodontal diseases: A review. *African J Microbiol Res*. 2015;9(48):2300–6.
48. Regeneration P. Academy Report 2005;1601–22.

49. Costa PF, Vaquette C, Zhang Q, Reis RL, Ivanovski S, Hutmacher DW. Advanced tissue engineering scaffold design for regeneration of the complex hierarchical periodontal structure. *J Clin Periodontol* 2014;41(3):283–94.
50. Laurell L, Gottlow J. Guided tissue regeneration update. *Int Dent J* 1998;48(1998):386-98.
51. Aurer A, JorgiE-Srdjak K. Membranes for Periodontal Regeneration. *Acta Stomatol Croat* 2005;39(1):107-12.
52. Singh AK. GTR membranes: The barriers for periodontal regeneration. *DHR-IJMS* 2013;4(1):31-8.
53. Sam G, Pillai BRM. Evolution of barrier membranes in periodontal regeneration-???are the third generation membranes really here?". *J Clin Diagnostic Res.* 2014;8(12):ZE14-ZE17.
54. Ogawa K, Miyaji H, Kato A, Kosen Y, Momose T, Yoshida T, et al. Periodontal tissue engineering by nano beta-tricalcium phosphate scaffold and fibroblast growth factor-2 in one-wall infrabony defects of dogs. *J Periodontal Res.* 2016;51(6):758-67.
55. Chen F-M, Jin Y. Periodontal tissue engineering and regeneration: current approaches and expanding opportunities. *Tissue Eng Part B Rev* 2010;16(2):219-55.
56. Wang J, Wang L, Zhou Z, Lai H, Xu P, Liao L, et al. Biodegradable polymer membranes applied in guided bone/tissue regeneration: A review. *Polymers* 2016;8(4):115.
57. Abou Neel EA, Chrzanowski W, Salih VM, Kim HW, Knowles JC. Tissue engineering in dentistry. *J Dent* 2014;42(8):915–28.

58. Yang F, Both SK, Yang X, Walboomers XF, Jansen JA. Development of an electrospun nano-apatite/PCL composite membrane for GTR/GBR application. *Acta Biomater* 2009;5(9):3295–304.
59. Bhardwaj N, Kundu SC. Electrospinning: A fascinating fiber fabrication technique. *Biotechnol Adv* 2010;28(3):325–47.
60. Agarwal S, Wendorff JH, Greiner A. Use of electrospinning technique for biomedical applications. *Polymer (Guildf)* 2008;49(26):5603–21.
61. Vonch J, Yarin a, Megaridis CM. Electrospinning: A study in the formation of nanofibers. *J Undergrad Res* 2007;1(1):1.
62. Chen H, Blitterswijk CVAN, Moroni L. Fabrication of nanofibrous scaffolds for tissue engineering applications. *Woodhead Publ Online*. 2013;
63. Zhang Y, Su B, Venugopal J, Ramakrishna S, Lim C. Biomimetic and bioactive nanofibrous scaffolds from electrospun composite nanofibers. *Int J Nanomedicine* 2007;1(9):623–38.
64. Goh Y-F, Shakir I, Hussain R. Electrospun fibers for tissue engineering, drug delivery, and wound dressing. *J Mater Sci* 2013;48(8):3027–54.
65. Pham QP, Sharma U, Mikos AG. Electrospinning of polymeric nanofibers for tissue engineering applications: a review. *Tissue Eng*. 2006;12(5):1197–211.
66. Shin S-H, Purevdorj O, Castano O, Planell J a, Kim H-W. A short review: Recent advances in electrospinning for bone tissue regeneration. *J Tissue Eng*. 2012;3(1):2041731412443530.

67. Hasan MM, Alam AKMM, Nayem KA. Application of Electrospinning Techniques for the Production of Tissue Engineering Scaffolds: a Review. *Eur Sci J*. 2014;10(15):1857-7881.
68. Athira KS, Sanpui P, Chatterjee K. Fabrication of Poly(Caprolactone) Nanofibers by Electrospinning. *J Polym Biopolym Phys Chem* 2014;2(4):62–6.
69. Dhandayuthapani B, Yoshida Y, Maekawa T, Kumar DS. Polymeric scaffolds in tissue engineering application: A review. *Int J Polym Sci* 2011. p.19.
70. Qian Y, Chen H, Xu Y, Yang J, Zhou X, Zhang F, et al. The preosteoblast response of electrospinning PLGA/PCL nanofibers: Effects of biomimetic architecture and collagen I. *Int J Nanomedicine*. 2016;11:4157–71.
71. Joseph D. Evaluating the Potential of Electrospun Membranes for Tissue Specific Signal Delivery in Cartilage and Bone Tissue Engineering. 2013.

ANNEXURE

Annexure 1

Dr.Hari Krishna Varma

Scientist in Charge

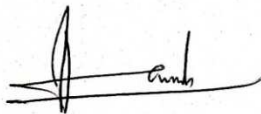
Bioceramic Laboratory

Sree Chitra Tirunal Institute for Medical Sciences and Technology

Trivandrum

To whomsoever in may concern

I will be happy to collaborate in developing and characterizing electro spun nano fibers for the fulfillment of MDS thesis entitled "Fabrication and invitro characterization of bioactive glass/nano-hydroxyapatite reinforced electrospun polycaprolactone composite membranes for periodontal tissue engineering" of Dr. Vishnu JS, Department of Periodontics and Oral implantology, Sree Mookambika Institute of Dental Sciences, Kulasekharam



Thanking you

DR.H.K.Varma

3-10-2015

Dr. P.R. HARIKRISHNA VARMA Ph.D.
Scientist in Charge, Bioceramics & SEM Laboratories
Biomedical Technology Wing
Sree Chitra Tirunal Institute of Medical Sciences and Technology
Poojappura, Thiruvananthapuram-695 012

SREE MOOKAMBIKA INSTITUTE OF DENTAL SCIENCES
KULASEKHARAM, KANYAKUMARI DIST., TAMIL NADU, INDIA.



INSTITUTIONAL RESEARCH COMMITTEE

Certificate

This is to certify that the research project protocol,
Ref no. 06/06/2015 titled, "*Fabrication and invitro characterization of bioactive glass/nano-hydroxyapatite reinforced electrospun polycaprolactone composite membranes for periodontal tissue engineering*" submitted by *Dr. Vishnu J.S., II Year MDS, Department of Periodontics and Oral Implantology* has been approved by the Institutional Research Committee at its meeting held on *15th June 2015*

Convener
Dr. T. Sreelal

Secretary
Dr. Pradeesh Sathyan